The Pennsylvania State University

The Graduate School

Department of Physiology

EXTRACTION AND BINDING CHARACTERIZATION OF HYALURONIC ACID BINDING PROTEINS FROM BOVINE NASAL CARTILAGE

A Thesis in

Physiology

by

Bret M. Weaver

Submitted in Partial Fulfillment
of the Requirements
for the Degree of

Master of Science

August 2009

The thesis of Bret M. Weaver was reviewed and approved* by the following:

Herbert H. Lipowsky
Professor and Head Dept. of Bioengineering
Thesis Advisor

William Hancock
Associate Professor of Bioengineering

Donna Korzick
Professor of Kinesiology
Chair, Physiology Program

*Signatures are on file in the Graduate School

ABSTRACT

The current project was undertaken to optimize the extraction of hyaluronic-acid binding proteins (HABPs) from bovine nasal cartilage (BNC). An incubation pull-down assay was devised by mixing various concentrations of trypsinized BNC with a constant amount of functionalized sepharose beads conjugated with hyaluronic acid (HA). Following incubation of BNC digests with the HA-derived beads, a fractional binding profile was established for a range of digest-to-bead proportions. Elution of the beads with 2M NaCl and 4M GCl showed most HABP binding activity coming off with 2M NaCl. Total protein and fractional binding values were determined with Bradford assay and SDS-PAGE electrophoresis, respectively. From these results, a mass elution scheme was prepared to follow a step-wise washing pattern proportional to ionic strength. This allowed protein yield and specific binding amounts to be calculated.

Conjugation efficiency of the derived sepharose beads was determined by measuring the difference in refractive index (RI) between the supernatant and the initial solution concentration of added 64kDa HA. The refractive indices of a stock solution of HA were used to construct a standard curve to calculate HA (w/v) % of the supernatant. Calculation of HABP binding values was determined using the protein concentrations eluted with 2M NaCl as they were found to be statistically more significant than the 4M GCl rinses ($P<0.01$).

A minimum of three percent conjugation was calculated from a standard conjugation assay with non-degraded 64kDa HA and functionalized sepharose beads. Trypsinized HABPs from BNC were found to have a $\overline{MW_w}$ of 53.4 kDa, a Kd of 7.235×10^{-8}M and a total binding-site concentration ([TBS]) of 1.775×10^{-6}M with most of the binding activity residing in the 47kDa link protein. Total specific binding activity gave a yield of 1.18% deduced from the mass-elution procedure.

The current project was focused around methods and results previously reported (Tengblad, 1978). Using conventional liquid affinity chromatography, specific binding activity was washed out in the 4M GCl fraction. Two species are commonly found to bind to HA after being extracted from trypsinized BNC: a 45kDa link protein and a 90kDa proteoglycan monomer. Three bands were analyzed with the current incubation pull-down method that contributed to the overall calculation of the weighted molecular-weight average: 97kDa, 65kDa and 47kDa. This approach was derived from previous reports, and MW differences were due to the higher concentration of acrylamide used to run the reducing PAGE. Liquid chromatography remains to be the best procedure in order to enhance the purity of the sample for proper in-vivo experimentation and interpretation of conjugative biochemical results.

TABLE OF CONTENTS

LIST OF FIGURES

LIST OF TABLES

ACKNOWLEDGEMENTS

I would like to sincerely thank Dr. Lipowsky for his driving wisdom, patience and financial support to conduct this project. He is my Yoda: "…you gotta keep your eye on the donut, 'cause in the end we'll all be pushing up daisies…" -Dr. Lipowsky

Chapter 1

Background and Introduction

1.1 Identifying the Source

Proteoglycan biochemistry and glycobiology is a rapidly growing field that is quickly covering a vast array of scientific disciplines. Not only has its role been well established within biochemical methodology, but the well appreciated physiochemical nature of proteoglycan interactions deduced from such studies are currently being applied to in-vivo models. The pericellular glycocalyx in its simplest form describes a meshwork of interconnected protein and glycosaminoglycan components that aggregate and form an exchangeable communicative environment between the intra and extracellular world. Many studies have been undertaken to elucidate the relationship between specific players of the extracellular glycocalyx and downstream intracellular events that effect a response to a local external cue. Syndecan is a proteoglycan that is composed of a linear protein core glycosylated with GAG (Glycos-Amino-Glycan) groups at selected Ser residues. The residues glycosylated depends on the primary sequence structure of the protein. It is produced, shuttled and modified along the ER-Golgi pathway to be secreted at the apical membrane site. This proteoglycan projects from the percicellular surface and interacts with other players of the ECM environment, and many studies have shown a direct link of syndecan-mediated signaling to manifest an intracellular response. This includes both the integration of transcription-dependent signaling cascades and cytoskeleton rearrangement, which leads into mechanotransducion. These studies are beyond the scope of the current one, but are worth mentioning.

Syndecan proteoglycans have three distinct domains: a linear core to which both keratin sulfate and chondroitin sulfate are O-covalently attached determining the overall heterogeneity of the proteoglycan, and two areas that lack these substituted GAG groups for non-covalent association with the surrounding glycocalyx. One is for binding HA link proteins to bridge its connection with HA, and another at the N-terminal domain that binds with the HA linear chain (Keiser, 1977). Together in associative conditions, the HA linear chain, link proteins and PG subunits aggregate to form an extractable fraction known as aggrecan. This can be harvested from cartilage such as bovine nasal septa that provided the source for extracting viable hyaluronic acid binding proteins (HABPs). Shown below is the natural turnover cycle of aggrecan in human articular cartilage (Fig 1). The same scheme can be applied in bovine species with the aggrecan product located at the apex. The smaller arrows show degradation sites along the PG subunit downstream from the HABP total binding area (N-termini of PG subunit and Link Protein (LP)).

1.1.1 Fig. 1: Cartoon schematic of Aggrecan production and turnover.

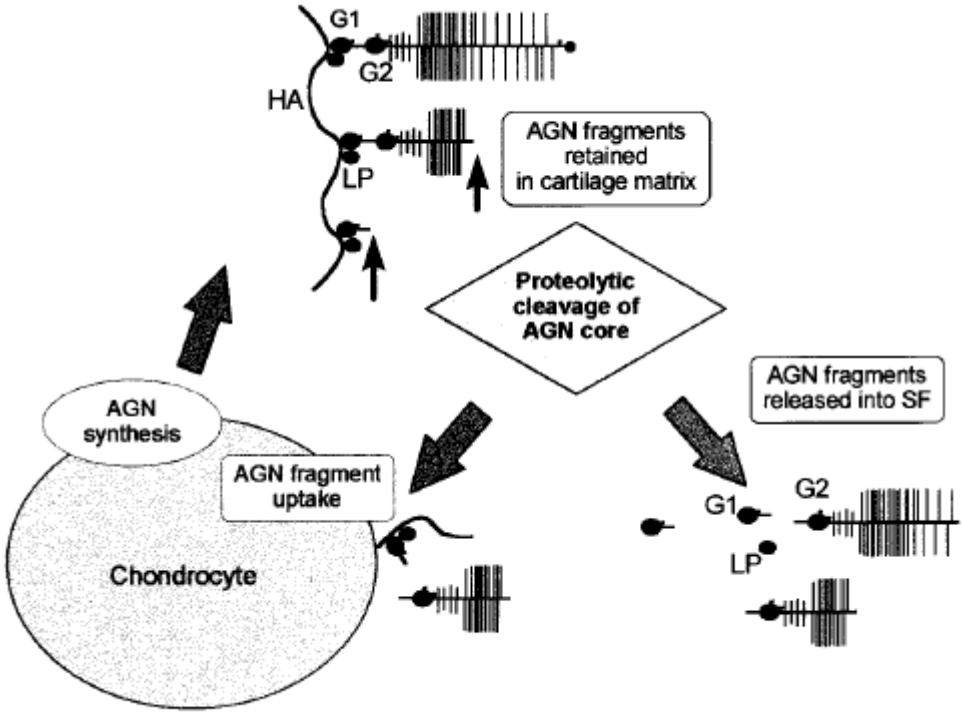

1.1.1 Fig 1: Cartoon schematic showing turnover cycle of aggrecan and its integrated components between the chondrocyte and extracellular matrix. From: Lark et. al., 1997

The importance of trying to visualize a specific ECM player along the vascular lumen and its plausible role to mediate an in-vivo response is growing with every report of diabetes and other aberrant inflammatory conditions, both acute and chronic. Examples include sepsis and systemic lupus erythematous. (SLE), respectively. In-vivo binding markers can be conjugated with HABPs harvested from cartilage to help understand these diseases more specifically in order to elucidate the normal dynamic intermolecular state along the vascular lumen endothelium.

1.2 Bio- and Physiochemical Association of Hyaluronic Acid

Hyaluronic acid is a glycoaminoglycan composed of the repeating subunit [-D-glucuronic acid (1-β-3) N-acetyl-D-Glucosamine (1-β-4) -] n. At physiological conditions, the molecule is fully ionized and the successive beta-bonds along the chain's length impart a coiling superstructure that can be related to the natural architecture of DNA. These two properties along with its increasing length up to $2x10^6$ Da in some tissues gives the molecule it's hygroscopic and viscoelastic nature. A large amount of HA is synthesized in articular cartilage of high molecular weight. This makes the internal joint surface amenable to impact stress which can be denuded by chronic arthritis. Smaller molecular weight species are found in tracheal cartilage which is essentially a resilient semi-solid tunnel for maintaining proper airflow to the lungs. As will be shown later, HA's perfect physiochemistry make it very difficult for the molecule to conjugate to $–NH_2$-functionalized substrates such as protein and sepharose beads. Using 13C and proton NMR spectroscopy, tertiary domains can be found with larger molecular weight species at high concentrations where the chain forms hairpins upon itself, and the $–COO^-$ group at one arbitrary site can H-bond with the N-acetyl group at another (Scott, et.al., 1999). This would then block substrate conjugation, and relatively smaller HA molecules would be needed to enhance the transitional rate.

HA is synthesized at the inside surface of the apical plasma membrane. Three isozymes have been identified: HAS1, 2 and 3. HAS2 is primarily responsible for producing and secreting the larger molecular weight forms.

This mechanism differs from the synthesis of other GAGs such as keratin sulfate, dermatin sulfate and chondroitin sulfate which are produced and subsequently modified against a protein core along the ER-Golgi secretory pathway. However, both types share the source of UDP high energy donors from the uronic acid metabolic pathway that begins with the modification of glucose-6-phosphate. These are sequestered from the cytoplasm, and for the case of HA synthesis are directly added at their reducing end by HAS at the inner leaflet of the periplasm. Inflammatory cytokines and various growth factors have been implicated in regulating this initial flux, but HASs themselves seem to be the constitutive ushers to provide a route for HA production and secretion. The supply of glucose-6-phosphate is the initial rate-limiting step in glycolysis which primes other pathways such as: the pentose-phosphate pathway that provides $NADH_2$ reducing equivalents for fatty acid production, glycogenesis in liver and muscle and the regulation of gluconeogenesis in non-fed states. Simply put the ability of HA and other GAGs to be produced and secreted depends on the availability of metabolic glucose and overall energy balance.

1.3 The HABP Binding Domain and its Relationship with HABP Isoforms

For all functional and structural purposes, hyaluronic acid binding proteins are virtually identical across the animal kingdom. Any differences among published reports may be attributed to the way binding fragments are generated, isolated and treated for analysis. The globular binding domains of HABPs and cartilage link proteins are non-glycosylated. cDNA molecular methods show sequence homology between link proteins and proteoglycan binding regions which are composed of a tandem array of alpha-helices and beta-pleated sheets adjoined by disulfide cross-bridges (Doege et. al., 1986)

Favorable thermodynamic non-covalent association at the binding interface between HABPs and hyaluronic acid would then be limited to the proper physiochemical orientation of the protein binding site and repetitive GAG subunits of the HA polymer. As discussed before, HA is composed of a predictable linear sequence of glucuronic acid and N-acetyl glucosamine. Any variation in the presentation to the protein binding surface would be due to MW and concentration at physiological pH. Optimal binding occurs within the range of pH 5 and 7 (Tengblad, 1981). At the same solution conditions, the HABP binding domain achieves its lowest Gibbs' free energy state. This ultimately comes down to the primary sequence in protein structure, and the aliphatic non-polar and polyanionic nature of HA must complementarily align with active site of HABPs.

When assessing the composition of isolated binding protein fractions from trypsinized extracts, four analytical features are consistently shown: a relatively equal amount of the basic amino-acid residues (BAA) Arg and Lys, an AA ratio between Cys and those BAAs of approximately 1:3, a low amount of GAG leftovers after isolation as determined by hexauronate analysis and a low amount of hydroxyproline content which designates the presence of collagen. Acetylating reagents such as dansyl chloride show eighty-percent binding inhibition compared with acetic anhydride in specifically targeting primary amino groups presented by the amino acid residues Lys and Arg (Heinegaard and Hascall, 1978). This is a highlighting mark with using cartilage as a source for binding protein. Of course, some sulfated GAG remnants that co-precipitate with variable Ser content are expected when initially extracting the binding fraction from the whole tissue.

The HABP globular binding domain is best conceptualized in the context of the four factors listed above in order to maintain a proper tertiary three dimensional form in solution at optimal pH. This is clearly evident when analyzing the structural binding properties of the link module (Kohda, et. al. 1996; Goetinck, et.al. 1987), and the trypsinized fraction is well characterized (Heinegaard and Hascall, 1974).

1.3.1 Impetus for Molecular Studies

HABPs isolated from tissue extracts have been done using conventional biochemical methods as will be explained in section 1.1.4. When the binding species is purified one can use cDNA and amino-acid sequencing analysis, and interface those results with a queried database that reference other isoforms and species-related HABPs. CD44, also known as the lymphocyte homing receptor, is a surface glycoprotein primarily expressed on epithelial and myeloid cell-types and has been shown to mediate T-cell activation, extravasation and margination, and lamellipodia outgrowth. This effectively maturates the inflammatory response (Oliferenko et.al., 2000; Turley et. al., 1991; Stamenkovic et. al., 1989; Siegelman et.al., 1999; Lesley et.al., 1994; Stamenkovic et.al., 1991; Culty et.al., 1990; Roscic-Mrkic, 2003). CD44v (polymorphic splice variants) are expressed in lymphoid tumor cells (Bartolazzi et.al., 1995). The expression mechanism may depend on adjoining variable exon sites much like antibody and TCR secretion, but the splicing-dependent machinery has not been well founded (Doege et.al., 1986). These variable isoforms are present in the supernatant and on the cell surface of tumor cells, and are probably responsible for disaggregating and disrupting the normal HA-PG arrangement to increase spreading, invasion and metastasis. The loss of physical integrity and controlled permeation properties along the endothelial glycocalyx that would result from this disruption can be supported by the resulting intermolecular charge modification (Paul et. al., 2005) and shunted equilibrium from HA and native HABPs (Fig. 2)

1.3.2 Fig 2: Rate Association Binding Kinetics Between HA and HABPs

$$[HA] + [BP] \underset{k_r}{\overset{k_f}{\rightleftharpoons}} [HA:BP]$$

$Rate_1 = k_f[HA][BP]$ $\quad$ $Rate_2 = k_r[HA:BP]$

At equilibrium: $Rate_1 = Rate_2 \Rightarrow K_d = [HA][BP]/[HA:BP] = k_r/k_f$. Variant binding factors infiltrating the glycocalyx and associating with HA increases $Rate_2$ by decreasing the functional native concentration of HA:BP. This leads to its dissociation and collapse of the luminal surface endothelium. HA occupies approximately fifty percent of the glycocalyx volume (Henry et. al., 1999), so its reasonable to assume a high probability of HA:BP break-down facilitated by these variant isoforms. Generating hybrid cDNA constructs helps differentiate HA attachment, and would therefore assess malignancy in pathological states (Bartolazzi et.al., 1995).

The non-pathological in-vivo HA-binding model initiates an autocrine-dependent intracellular signaling cascade, and parallels the role of other HABP isoforms such as RHAMM (Receptor for Hyaluronic Acid Mediated Motility) (Singleton et.al., 2002; Bourguignon et.al, 1999; Goueffic et.al., 2006). Together it seems CD44 and related isoforms effect and possibly regulate the overall response to antigen clearance and tissue maintenance. HABPs harvested from bovine nasal cartilage present similar amino-acid profiles and must maintain the same proper three-dimensional fold at the binding surface. Any system used to express HA binding antigens or isoforms needs to be put in context. If the species is glycosylated, yeast would be a better model than bacteria (i.e. E.coli) unless the expressed protein itself is sufficient. Such experiments depend on the targeted sequence, potency and requisite glycosylation pattern. However, proper steps need to be followed to ensure LPS and related antigens are free of the purified HABP binding fraction. This would otherwise lead to an unwanted inflammatory state in in-vivo injection experiments.

1.4 Traditional Methods and Parameters Used to Isolate and Characterize Binding Fractions

All biochemical studies investigated to harvest and purify the HABP binding fraction from its relevant tissue source encompass a number of strategies that define and quantify the intrinsic physiochemical parameters of HA and associated proteins. This project is a straightforward process of harvesting HABP binding activity from a crude extract of trypsinized bovine nasal cartilage. As will be discussed later, identifying specific binding species depends on using procedures that eliminate non-specific interference.

1.4.1 CsCl Gradient

This is probably the most efficient means of isolating the functional binding fraction aggrecan from cartilage. By their nature, proteoglycans are polydisperse in molecular weight and structure. This would then lead to a proper decision in their mass isolation using centrifugal techniques. Buoyant density is a measure of an object's ability to float. A fraction having a large buoyant density displaces more aqueous volume than its own weight. In associative conditions (0.4M GCl, pH 5-7) a CsCl density gradient of approximately 1.7g/ml is used to collect the A1 fraction (protein polysaccharide complex (PPC)) spun at 40000rpm excluding non-specific binding fragments such as collagen to the top of the tube (Sajdera and Hascall, 1969). The A1 complex is easily pelleted to the bottom of the tube. The PPC is then disrupted in 4M GCl at a gradient of 1.5-1.6 g/ml spun at the same rate. This solubilizes the complex and the HABP binding fraction can be easily extracted from the top of the dissociative gradient and further characterized for amino acid content and binding ability (Hascall and Sajderra, 1968). The top fraction is mainly composed of protein while the bottom fraction has a high proportion of both protein and uronate due to the segregation of proteoglycan content.

It is hard to know where HA equilibrates along the dissociative gradient without knowing its MW, but when the bottom and top fractions are re-combined aggregation is evident.

This can be followed up by chromatography, which will be discussed in 1.4.2. The top fraction is relatively low in hydroxyproline, has about the same number of BAARs (Basic Amino Acid Residues), low in Ser which rules out glycosylated protein, and shows a 1:3 to 1:4 ratio in Cys:BAA content. This is systematic proof for the presence of HABPs harvested from bovine nasal cartilage using simple associative-dissociative CsCl gradient centrifugation.

1.4.2 Column Chromatography and Combined Enzymatic Analysis

The proteoglycan constituents of intact cartilage are well-manifested by the sequential steps needed to purify binding proteins. This project was mainly geared around prescribed procedures that yield a specific binding fraction of 2.5% using affinity chromatography (Tengblad, 1978), Immunochemistry experiments using antibodies against hyaluronidase-prepared fractions is evidence for multiple binding antigens (Keiser, 1982). The observation of other studies showing results pertaining to the complex heterogeneity of this type of tissue needs to be appreciated. These concepts and useful biochemical strategies to analyze harvested tissue will be succinctly discussed here. All literature sources that provide a knowledgeable foundation for this project will be cited in detail among the list of references.

1.4.2.1 Relevant Distillation from Previous Work

The immunogenicity of PG fractions can be differentiated by the degree and extent to which they are glycosylated. This presents the PG core protein surface in uniquely recognizable ways, hence generating epitope variability. When these fractions are degraded by selective enzymes such as Chondroitinase and Hyaluronidase that target specific glycosidic residues, surface epitope expression becomes modulated and immunogenicity for the PG core components can be affected. Kinetic analysis shows the initial rate of HA degradation favored by HAse endo-glycosidases, but at increasing time intervals up to approximately 30mins, chondroitinase can be used to initially select out sulfated GAGs in the extract before HA becomes largely degraded. This increases the purity of the sample by keeping the functional binding complex intact.

The enzymatic discontinuity may be explained by the alternating differences in GAG sequence between CS and HA. HA is essentially a glycopolymer made up of repeating glucose subunits, while CS substitutes galactose at every other position along the chain. The axial vs. equatorial hydroxyl group at the fourth carbon between galactose and glucose may present differing stereoelectronic environments that increase or decrease the potential for nucleophilic attack at the anomeric carbon. Better chromatographic resolution and fractional characterization of the HABP derivatives from bovine nasal cartilage is achieved after degrading the initial crude extract with chondroitinase before trypsinization (Heinegard and Hascall, 1974). Two MW species were observed after the A1 fraction was isolated and treated from an associative CsCl gradient. The 90 kDa and a 45 kDa fractions eluted as separate peaks along a Sephadex G200 column under dissociative conditions with the 90kDa fraction having a lower K_{av}. The eluted fractions were appropriately named T-G200-2 and T-G200-3, corresponding with their respective K_{av} elution values (K_{av} (45kDa)>K_{av} (90kDa)). The 90kDa band on a SDS reducing PAGE was also more diffuse than the 45kDa band. This can be termed "PG spreading". These two reasons point out the buoyant density differences between glycans and pure HABPs. The heterogeneity of substituted glycans give a lower buoyant density than pure HABPs in a dissociative CsCl gradient. The tandem approach of using associative-dissociative CsCl gradient centrifugation to initially extract the A1 aggregate before conjunctive enzymatic glycosidic degradation augments specificity and leads to further procedures that characterize their functional capacity such as ELISA, Western Blots and Immunoprecipitation. Competitive binding studies against a standard preparation can be used to deduce the potency of the binding fraction prepared along this scheme. Using reducing and alkylation agents to target Cys and BAA residues should be implemented to interfere with the protein's native conformation and potential to bind to HA substrates. Observing a decrease in binding ability after this treatment would be substantial to say a good extract has been harvested.

1.5 Foundation for the Current Project

Four points can be made from the preceding introduction that provide a means of developing an experiment to effectively analyze the yield of harvested HABPs from trypsinized bovine nasal cartilage:

1. A defining presence of BAARs. This enables the use of a Bradford assay in determining functional protein amount. Undisclosed results from an accompanying experiment along with this project show increased BAAR liberation during HAse incubation with crude extract in a time dependent fashion. Maximum absorbance was found at 2hr out of an 8hr incubation period. Toward the end of this time frame, a minimal absorbance was seen which can be explained by the increasing presence of smaller HA derivatives that seem to saturate the enzymatic site under conditions of low ionic strength (Asteriou et. al, 2005).
2. Multiple binding species. This has been shown with immunochemistry experiments using agarose diffusion procedures to observe several precipitation lines between the prepared fractions and antibodies against isolated binding antigens.
3. Characteristically low yield in specific binding activity after eluting bound substrate with salts such as NaCl and GCl.
4. Molecular weight of HA. Tertiary domain organization of HMW forms under high concentration may block the repetitive carboxyl group from conjugating to the amino group of the selected substrate.

Chapter 2

Materials and Methods

2.1 Tissue Processing

Bovine nasal cartilage was extracted from the decapitated heads of slaughtered cows at the PSU meat lab facility and had a net tissue weight of 60g. Stiff pliers were used to separate associated membranes before weighing and processing of the cartilage. It was grated with a Surform pocket plane and dissolved in 4M Guanidium Chloride(GCl)/0.5M Sodium Acetate (NaAc); pH 5.8 at 4^{o}C for 30 hr with constant stirring according to prescribed procedures (Tengblad, 1978). One milliliter aliquots were taken at various time-points, spun and dialyzed. The Bradford assay was used to monitor solubilized protein levels which were found to plateau at 30hr. [Fig 6, Step 1] (Fig 3).

2.1.1 Fig 3: Solubilized Protein Levels of BNC through 30hr Incubation with 4M GCl

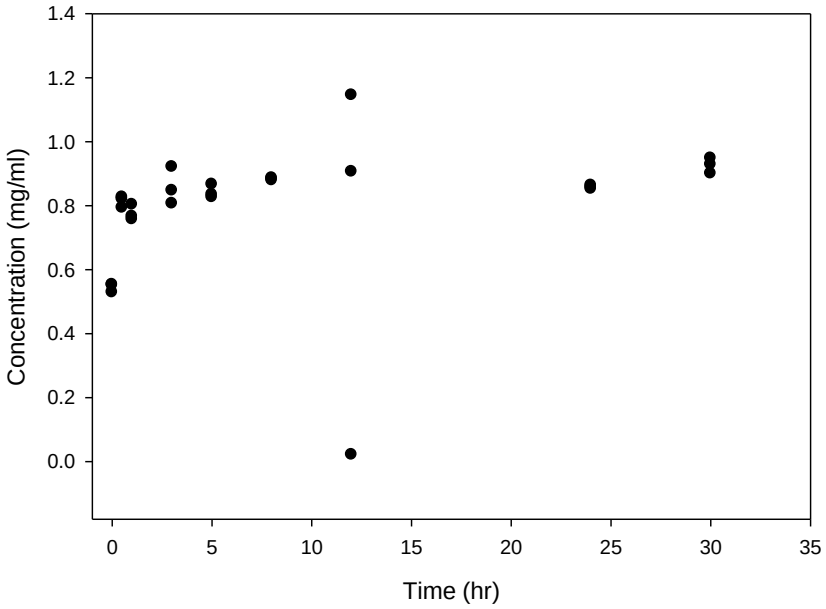

Fig 3: Solubilized proteins levels were measured from 1ml aliquots at various time-points through 30hr incubation with 4M GCl in triplicate. The results show the maximum amount of protein coming off in solution at 30hr. .

GCl is a very dense salt, so the buffer was titrated with enough deionized water to solubilize it before bringing the total solution to the appropriate volume. After filtering the extract with pre-washed cheesecloth, it was maximally dialyzed (12 kDa MWCO, Sigma) in deionized water for 24hr, then with 0.1MTris/0.1M NaAc; pH 7.3 for 12hr on a shaker table at 4^{o}C. The buffered extract was frozen in 50ml parcels at -20^{o}C until further use[Fig 6, Step 2]. All tools and surfaces were sterile, and gloves were used at all times during this process.

2.2 Bead Saturation

Lyophilized hyaluronate (HA) from human umbilical cord (LIfecore Biomed, 64kDa) was conjugated with NH_2-functionalized sepharose beads (Affigel 102, BioRad, Hercules, CA) according to established procedures (Underhill and Zhang). A total of 0.5g 64kDa HA was used with 25ml of minimally saturated and equilibrated beads. A conjugation assay was performed to assess the relative amounts of beads and HA needed to achieve maximum conjugation and bead saturation.

A 2.4% HA (2.4g/100ml deionized water) stock solution was prepared for all procedures. This was the highest concentration achievable using a 15 ml 10 MWCO filter (Millipore). The limitation may be due to the high saturating potential of HA and its increase in viscosity proportional to concentration. The beads were equilibrated in a 5ml syringe with a 0.2u filter (Acrodisc, 0.2um HT Tuffryn Membrane;Pall, Gelman Laboratory) using 25mM phosphate buffer, pH 5 according to package insert. Several washings with the buffer were required to remove sodium azide in the stock preparation which was present as a bacteriostatic preservative. Azide is a nucleophile, hence the beads must be thoroughly washed to ensure non-interference in the conjugation process. For this same reason, Tris and Acetate buffers were not used in order to prevent unwanted amino and acetyl substitution, respectively.

The conjugation buffer was prepared by the addition of the reagent carbodiimide (FW= 191.71, Sigma) to the phosphate equilibration buffer at a concentration of 5mM. When the beads are in their compact and minimally saturated form, the concentration of surface-terminal amino groups is approximated at 15 umol/ml. After equilibration, the beads were diluted 15x in the same buffer to a concentration of 1umol/ml. One ml of the final solution was added to six individual autoclaved glass tubes. The following amounts of HA were added to each tube from the stock solution: 100mg, 50mg, 20mg, 10mg, 5mg, and 1mg.

It was suggested by the manufacturer the solvent fraction of the total conjugation reaction be no greater than 0.3. Extra conjugation buffer was added to each reaction mixture to reduce the viscosity from added HA while maintaining the appropriate solvent fraction (Table 1).

2.2.1 Table 1: Fractional Volume Contribution by Added Buffer Related to Incubation Substituents

	Amount HA Added					
Substituent	1mg	5mg	10mg	20mg	50mg	100mg
64kDa HA; (from 2.367 % (w/v) stock	40ul	210ul	420 ul	840 ul	2.1 ml	4.2 ml
1 umol/mltNH2 Affigel (Dil 1/15x)	1ml	1ml	1ml	1ml	1 ml	1 ml
25 mM Phosphate Buffer; pH 4.7	300ul	360ul	420 ul	550 ul	1.93 ml	2.56 ml
Fractional Contribution of Buffer	0.22	0.23	0.23	0.23	0.38	0.33

All tubes were incubated at 37^{o}C for 3hrs with constant shaking. The tubes were placed at an angle with the bottom of the incubator to ensure mixing without displacing the majority of the beads from the solution. If the inside surfaces of the tubes are largely coated with beads, then the mixture is being shaken too rapidly and conjugation will not be complete. After incubation, the tubes were cooled to room temperature and spun at 3000g for 30min. Refractive indices (RI) were measured from 100ul of the supernatant using the Leica ABBE Mark II refractometer (Model 10480) and measurements from at least five aliquots were used to attain an average RI per tube. The difference between these averaged readings and the conjugation buffer gave the change in RI from the solvent due to the remaining HA in solution that was not conjugated. The amount of HA left in the supernatant was determined from the a standard RI curve constructed from the stock solution (Fig 4, 5).

2.2.2 Fig 4: Standard Curve of dRI in Terms of HA Fraction (w/v)

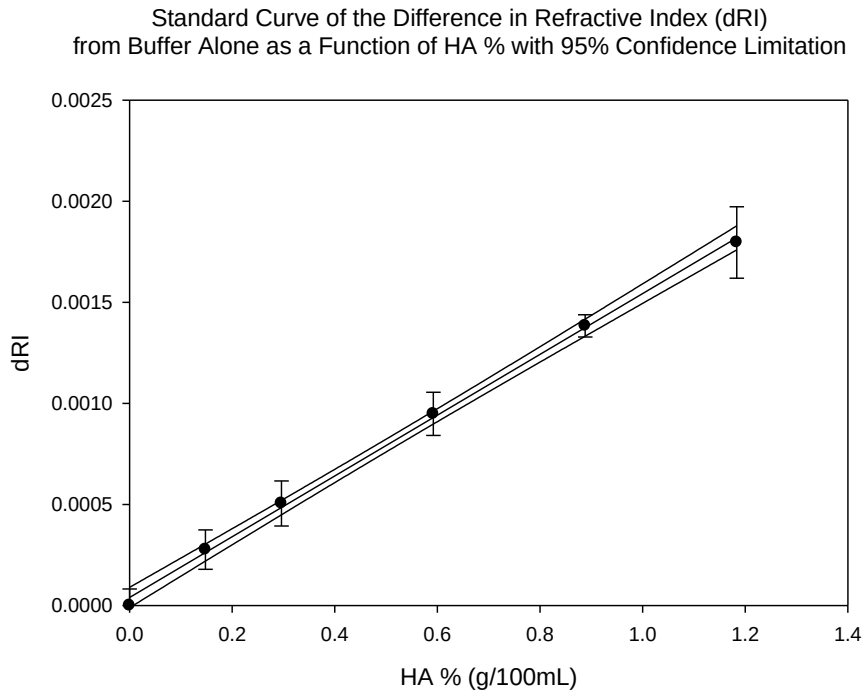

Fig 4: The difference in refractive index (dRI) plotted in terms of HA% (g/100ml). R^2=0.9987 and $p<0.001$.

2.2.3 Fig 5: Standard Curve of dRI in Terms of HA Fraction (w/v) corrected to zero intercept.

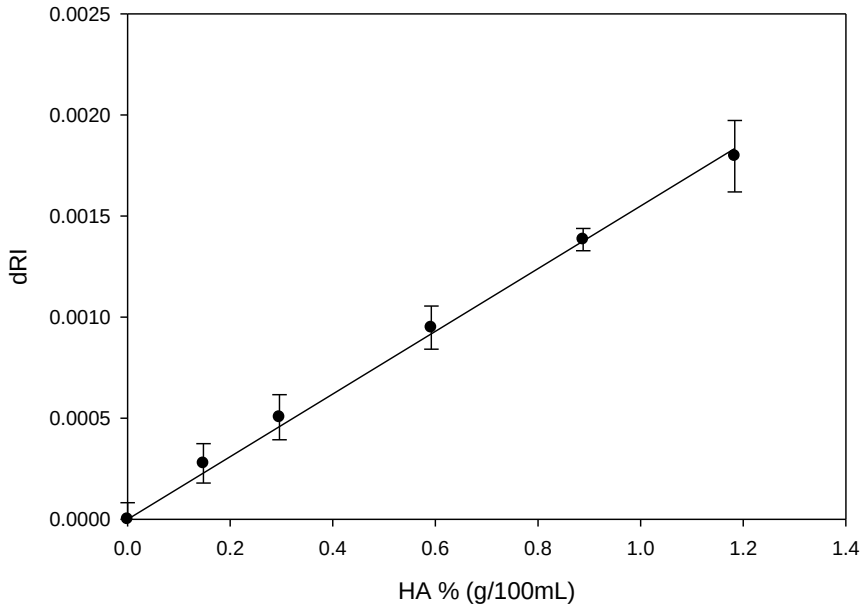

Fig 5: Correction of standard dRI curve to zero interception. The corrected slope falls within the deviation of individual values. Therefore, the equation: dRI=0.0015 ([HA%]) is a reliable model to predict the amount of HA in solution contributing to refractive index.

The buffer with carbodiimide showed no difference in RI than with buffer alone. Conjugation percentage was calculated with the following equation: $[(C_i-C_s)/C_i]x100$. C_i is the initial reaction concentration of HA in w/v (g/100ml), and C_s is the concentration of free HA remaining in the supernatant. Two conjugation profiles from the standard assay were created to assess the completion of the mass conjugation procedure using 0.5g HA (Underhill and Zhang).

This is assuming reaction completion depends on both of two independent factors: the mol/mol fraction between terminal amino groups present on the bead surface and HA in solution, and percent bead concentration in the conjugation mixture. These conditions constitute an entropically-dominant reactive state consistent with the physiochemical observations of HA explained in section 1.2. The bead concentration was calculated from the final dilution factor of the compact bead volume in each reaction tube.

2.3 Hyaluronic Acid Binding Protein (HABP) Binding Assay

An aliquot of untrypsinized frozen bovine nasal cartilage was thawed and concentrated using 10 kea MWCO centrifuge tubes (Centrals) by spinning at 3000xg to minimal volume at 4^{o}C[Fig 6, Step 3]. Half the extract was then digested with TPCK- treated trypsin (Sigma) at 2% w/w for 3hr at 37^{o}C with constant shaking. The reaction was stopped with soybean trypsin inhibitor (STI, Sigma) at 2x the molar weight of trypsin added and incubated overnight at room temperature with constant shaking[Fig 6, Step 4]. Both the trypsinized and untrypsinized extracts (TE and UTE, respectively) were diluted in series with cold 0.1M Tris/0.1M NaAcetate; pH 7.3 on ice at relative concentrations of 1 to 0.2, 1 being the most concentrated [Fig 6,Step 5]. The serial dilutions were done in 0.2 increments and corresponded to approximately 1.5mg/ml to 0.3mg/ml for TE, and 0.8mg/ml to 0.2mg/ml for UTE. All protein content measurements were determined with the Bradford assay using the Shimadzu Pharma Spectrophotometer UV-1700, and the accompanied Shimadzu UV Probe computer program. Standards were constructed with the appropriate solvent or buffer to control for ionic strength.

A pilot assay was first performed to determine the proper amounts of extract and beads to add to each binding incubation mixture. One-milliliter of saturated beads was added to undiluted UTE aliquots of 0.1, 0.25, 0.5, 1, 2 and 4ml. Only the first three treatments eluted protein in a proportional fashion.

This was attributed to both or one of two factors: 1.) an entropic effect of relative volumes between the extract and beads used where higher yields were obtained with tighter vol:vol ratios and 2.) possible bead aspiration when sucking off the supernatant. The final assay was conducted with both the UTE and TE at their respective series concentration [Fig 6,Step 5]. This also incorporated a blank incubation where only buffer was used. A constant volume ratio of 2ml of extract was added to 0.5ml of conjugated beads.

Beads were equilibrated with cold 0.1M Tris/0.1M NaAcetate pH 7.3 as previously mentioned. One-half milliliter aliquots were placed in separate ten milliliter autoclaved glass capped tubes. All tubes were vortexed slightly and allowed to settle overnight at 4^{o}C. The tubes were then spun at 3000xg for 30min at 4^{o}C and the unbound supernatant was collected using sterilized Pasteur pipettes [Fig 6, Step 6]. Protein content was determined on the supernatant with the Bradford assay using the Tris/Acetate buffer to conduct the standard. A series of wash steps then took place where 2ml ice cold 2M NaCl was used to wash each bead pellet, vortexed slightly and allowed to settle on ice for 30mins. The tubes were spun again at 3000xg for 30min at 4^{o}C, and protein content was determined on the supernatant using a 2M NaCl Bradford standard [Fig 6, Step 7]. After this fraction was collected, the beads were treated the same with the addition of ice cold 4M GCl [Fig 6, Step 8]. The 4M GCl elution fractions needed to be washed and concentrated with cold 0.15M NaCl in 0.5ml capped 10 MWCO eppindorf tubes (Fisher). They were spun at 3000xg to minimal volume. This was done to eliminate excess GCl that would interfere with the Bradford reagent, and to attain three replicate readings diluted from a workable concentration. According to Beer's Law, absorbance is proportional to the concentration. The unbound fraction and 2M NaCl eluted fractions were able to be read directly using the appropriate standard correcting for background absorbance.

The 4M GCl fractions, however needed to be measured with a 0.15M NaCl Bradford standard, and corrected for both background absorbance and the dilution factor used. In order to standardize the 4M GCl elution results, values needed to be calculated in terms of a two-milliliter elution volume. For example: if a measurement came from a 200ul concentrated sample that was diluted by 1/5, the final reading would be: (observed)*5*(0.2/2). The following figure shows the overall scheme to assay for the binding capacity of the trypsinized extract:

2.3.1 Fig.6: Flow scheme shown for initial tissue extraction and binding assay.

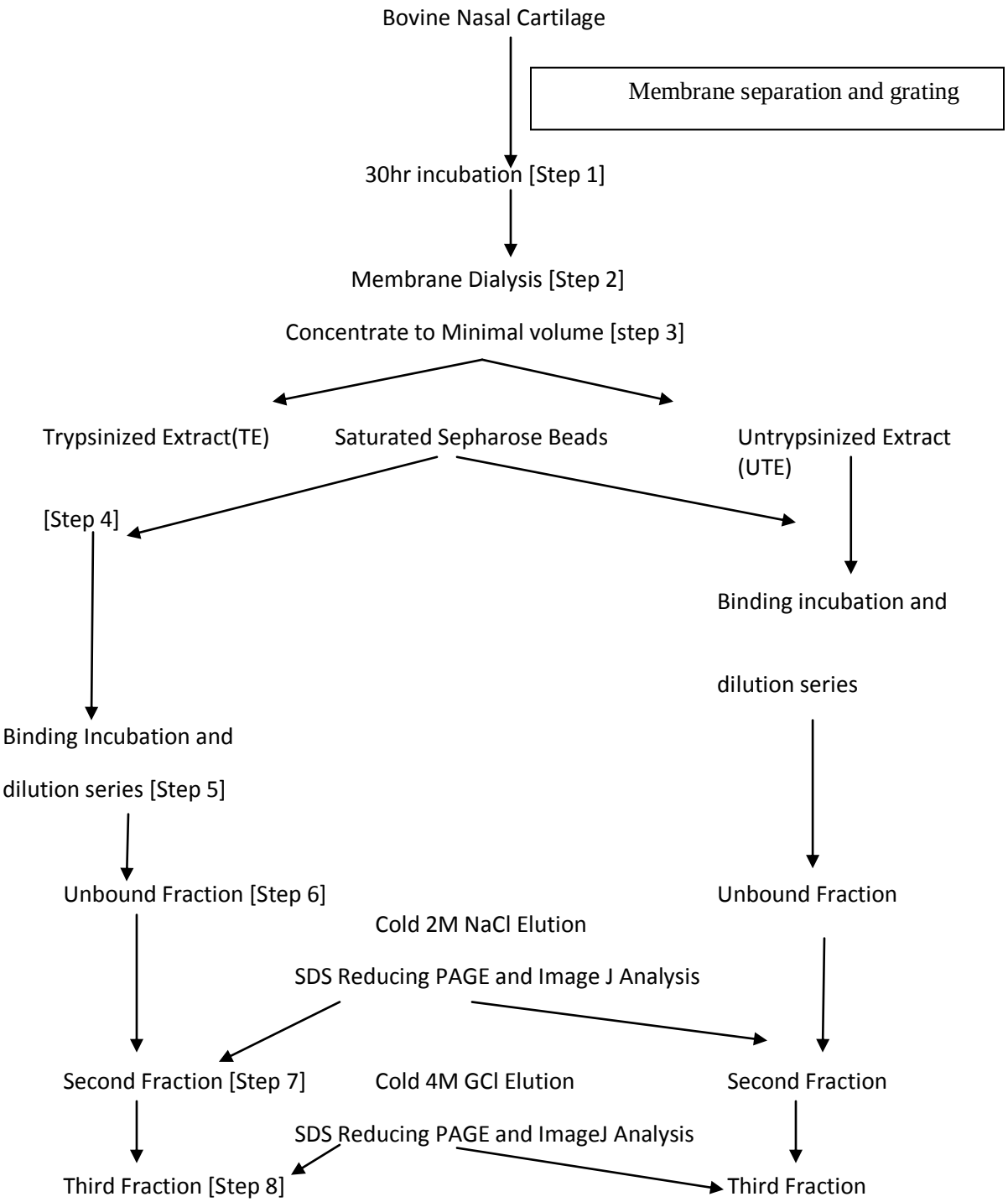

Fig. 6: Flow scheme shown for initial tissue extraction and binding assay. Details of Affigel-102 Sepharose conjugation are left out for simplicity.

2.3.2 HABP analysis

To visualize the eluted HABPs, a 15% SDS reducing PAGE stained with Coomassie blue R250 (Biolab, Hercules, CA) was used to empirically determine the fractional contribution of each species. A picture of the gels was taken and analyzed with the ImageJ software program. Images were taken with the Gel dot analyzer (Epichem Darkroom, UVP Bio Imaging Systems). Band intensities were determined for the TE binding assay. This was done by drawing a rectangle around each individual peak using SigmaPlot where each lateral side (width) was limited to half of the maximum peak intensity (height) (Fig 7).

2.3.2.1 Fig 7: Procedure to determine individual band intensities

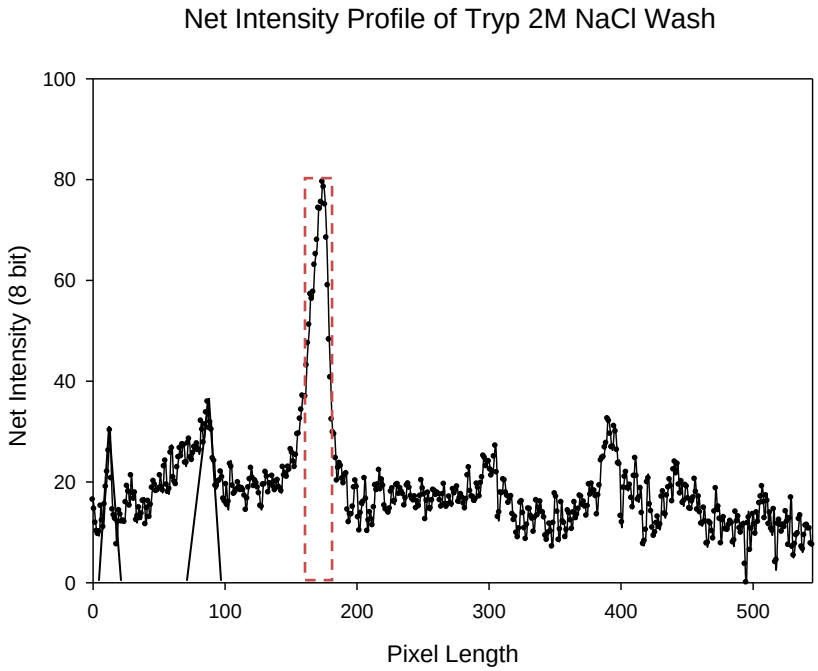

Fig 7: Procedure to determine individual band intensities. As seen with the 47kDa MW species, the band intensity was calculated by drawing a rectangle covering the individual peak where the height was limited to the net intensity of the band and the width to half of that value. The area of the rectangle (pixel length x net intensity) is proportional to the integrated band intensity. Background noise made it difficult to calculate the integrated intensity of the two bands running at 97 and 65 kDa, so a line was drawn tangent to the peak intersecting the ordinate in order to approximate half the individual peak intensity.

The area of the peak is proportional to the integrated band intensity. The total intensity of each individual lane was also determined using ImageJ. This is best conceptualized as the total area under the curve representing the analyzed pixel length down the ordinate of the intensity profile (Fig 7). The fractional peak intensity (integrated band intensity divided by the total intensity) gave the relative contribution of each molecular weight species coming off in each fraction. All values were corrected against the gel background. Determining the fractional peak intensities also helped in calculating the weighted molecular weight average between all species analyzed in each elution.

2.4 Mass Elution Scheme

An initial assay was conducted using 10ml of freshly concentrated TE incubated with 10ml conjugated beads. The total mixture was parceled into autoclaved glass tubes. Using both a 1:1 extract:bead volume ratio and glass tubes were needed to minimize bead loss while trying to realize an enhanced yield en-masse. The incubation buffer used was 0.1MTris/0.1M NaAcetate, pH 6.0. HABPs bind optimally between pH 5 and 7 (Tengblad, 1981). Earlier results showed most of the eluted protein came off with the 2M NaCl rinse and subsequently insignificant levels of protein were found in the 4M GCl elution fractions. With the current mass elution scheme, a step-wise rinsing pattern was conducted with 1M, 1.5M and 2M NaCl followed up by 4M GCl. The basis for this approach was to observe changes in specific binding activity as ionic strength incrementally increased in a step-wise manner.

After the extract was added, the mixture was vortexed slightly and the beads were allowed to settle on ice for 30mins. The tubes were then spun at 3000xg for 30mins at 4^{o}C. Two volumes each of 1M NaCl, 1.5M NaCl and 2M NaCl, and three volumes of 4M GCl were used to wash the beads at separate steps, and all eluants were pooled. An A280 assay was used to approximate the amount of total protein coming off the beads and an elution profile was created (Fig 8).

2.4.1 Fig 8: Mass elution profile following several volumes of selective ionic conditions

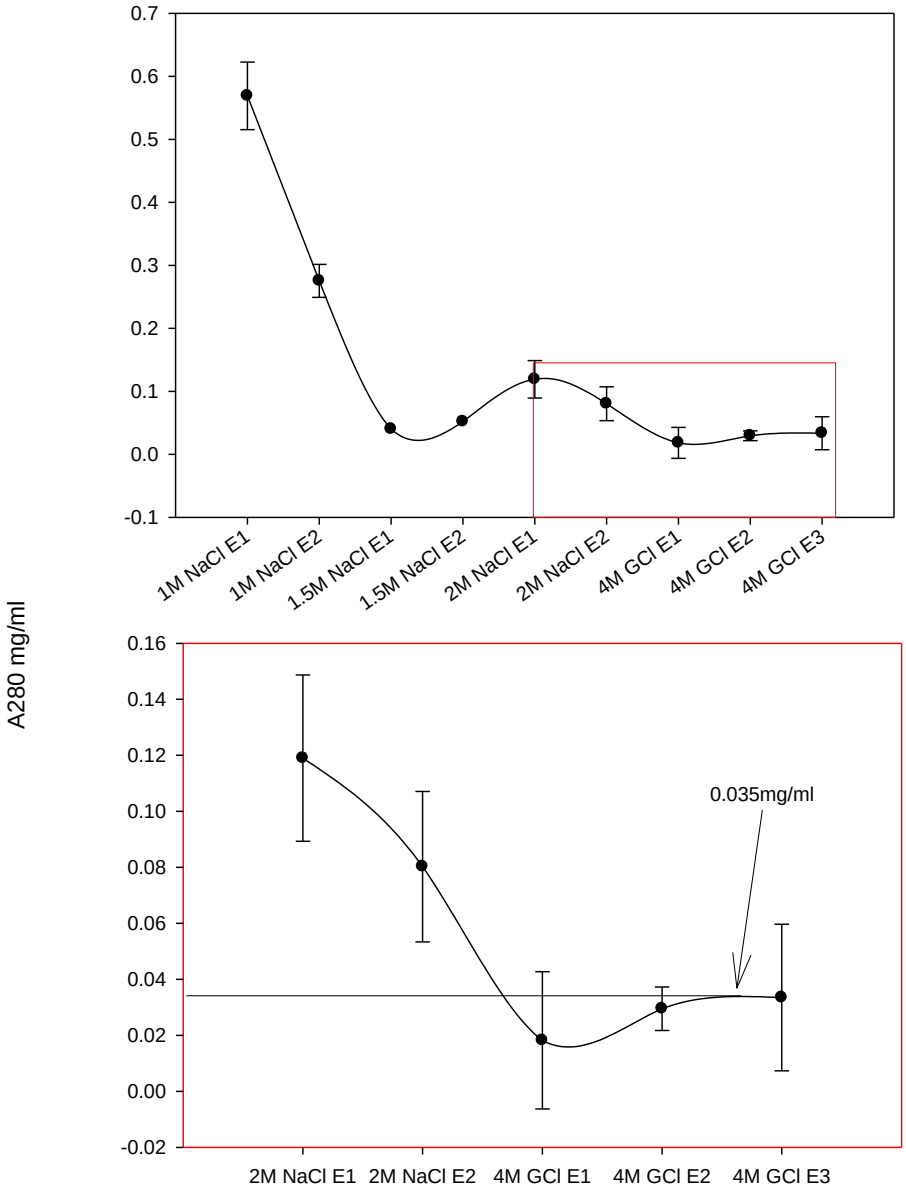

Fig 8: Mass elution profile following several volumes of selective ionic conditions. Upper panel shows scheme in its entirety from the first elution conditions. Bottom panel shows elution profile magnified from the first volume elution of 2M NaCl to the last volume elution of 4M GCl.

Separate A280 standards were not necessary during this process as in the binding assay. The GCl fractions were treated as before. All pooled fractions were spun down, concentrated and measurements were standardized to a 10ml elution volume.

After this initial assay, 200ml of trypsinized extract was processed en-masse. It was necessary to do the extraction in a series of multiple cycles with the limited volume of saturated beads available. GCl carried over if the beads were not thoroughly washed after each cycle. Three volumes of cold deionized water were used to rinse the beads before resetting them with an equal volume of 0.1MTris/0.1M NaAc, pH6. If a large amount of beads were used at one time during the GCl elution step the beads were aspirated when drawing off the supernatant. This was attributed to the increased viscosity of the 4M GCl solution and was confirmed by earlier studies (Kawahara and Tanford, 1966). The incubation mixture was parceled into separate glass tubes making sure the bead volume does not occupy a large fraction of the tubes. Based on the initial elution profile, a two-step mass elution scheme was conducted. Elution volumes were added in terms of the amount of molar salt needed to separate the desired protein product from a 1:1 bead:salt volume ratio. The profile followed 2 volumes of 1M NaCl, 2 volumes of 1.5M NaCl, 2 volumes of 2M NaCl and 3 volumes of 4M NaCl. With a 1:1 bead: salt ratio, 9 mol NaCl and 12 mol GCl per volume of conjugated beads were used to wash the bounded proteins in a two step fashion. The targeted protein product came off in the GCl fraction as seen with the Micheles-Menton plateau from 4M GCl E1 to 4M GCl E3 (Fig 8, lower panel) This fraction was pooled, concentrated and washed with cold deionized water using 10 kDa MWCO tubes spun to minimal volume at 3000xg at 4^{o}C. This was done to wash out all the excess salt that may saturate and damage the protein before being lyophilized or frozen for further use.

Chapter 3

Results

3.1 Initial Tissue Processing

Processed and grated cartilage tissue showed maximum protein levels after 30hr incubation with 4M GCl [Fig 6, Step 1](Fig 3). After trypsinizing the cartilage extract, three bands were prominently seen and analyzed for fractional binding contribution [Fig 9, Lane 5, arrows]. A 15% SDS reducing PAGE was run on trypsinized bovine nasal cartilage. Any bands migrating below 45kDa in the trypsinized lane was attributed to Soybean Trypsin Inhibitor (STI), Trypsin or protein content not known to bind to hyaluronic acid. This was confirmed by previous reports (Tengblad, 1978; Hascall and Heinegaard, 1974) Reducing conditions were proven to unaffect migrating distance to any significant degree (Hascall and Heinegaard, 1974). The relative Trypsin/STI amount added in Lane 6 was 1:2 in order to mimic the ratio added for BNC treatment. This controlled for any intensity differences seen in the trypsinized extract (Lane 5). No differences were seen.

3.1.1 Fig 9: 15% SDS-Reducing PAGE of Trypsinized Extract

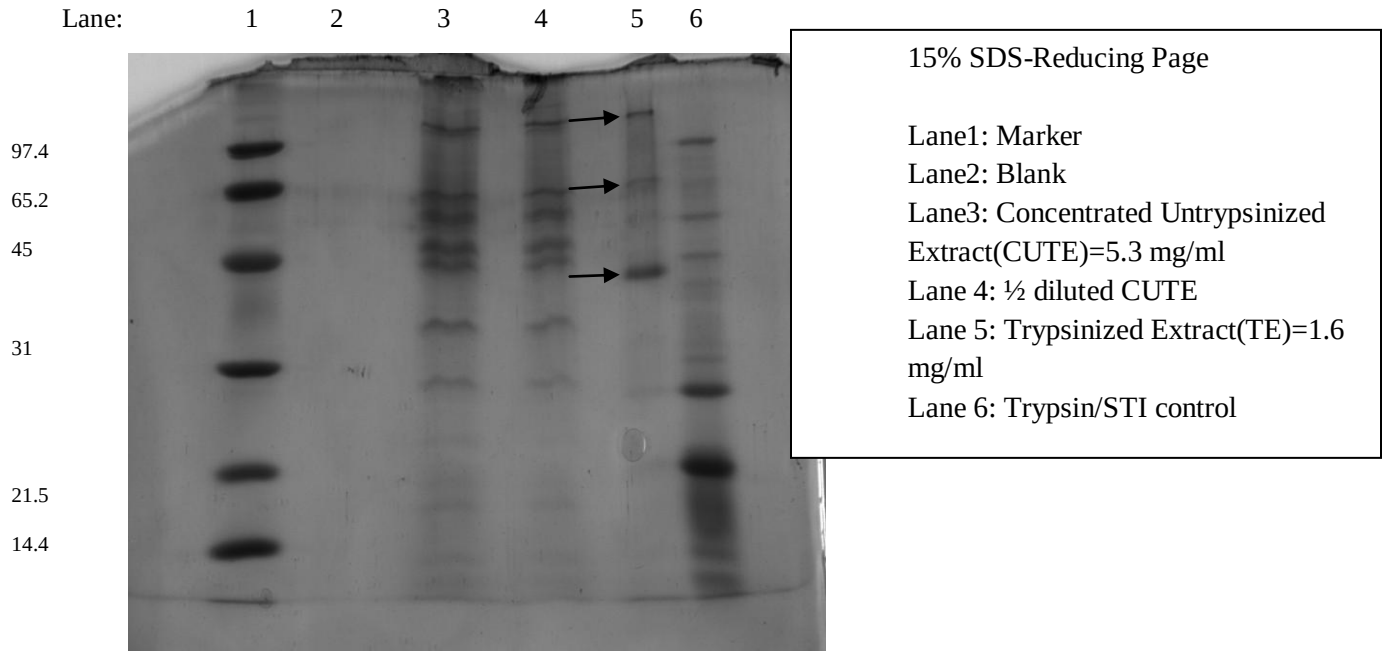

Fig 9: Lanes labeled left to right. Lane 1: Molecular Weight Marker. Values in kDa shown at left. Lane2: Blank Control. Lane 3: Concentrated Untrypsinzed Extract (CUE)=5.3mg/ml. Lane 4: CUE diluted by ½ to enhance clarity. Lane 5: Trypsinized Extract. Arrows show bands analyzed for fractional binding contribution. Concentration=1.6mg/ml. Lane 6: Trypsin/Soybean Trypsin Inhibitor (STI) Control.

3.2 Bead Saturation and HA Conjugation

A standard curve was constructed to predict the difference in refractive index based on the content of HA in solution (w/v, MW=64 kDa). Fig. 4 shows a linear curve ($P<0.001$, $R^2=0.9987$) within a 95% confidence interval and was subsequently corrected for zero interception (Fig 5). The equation dRI=0.0015(HA%) was used to calculate the amount of HA left in the supernatant post conjugation, and the formula $[(C_i-C_x)/C_i]x100$ was used to calculate conjugation percentage. Carbodiimide reagent was not shown to interfere with refraction (data not shown). A conjugation curve was generated from varying amounts of HA against a constant volume of amino-derived sepharose beads (see materials and methods).

Conjugation percent was plotted in terms of the relative mole ratio between terminal amino groups and HA (Fig. 10), and was shown to reach a maximum at approximately 50 (R^2=0.9376).

3.2.1 Fig 10: Conjugation Percentage of Amino-Derived Sepharose Beads with Hyaluronic Acid (HA)

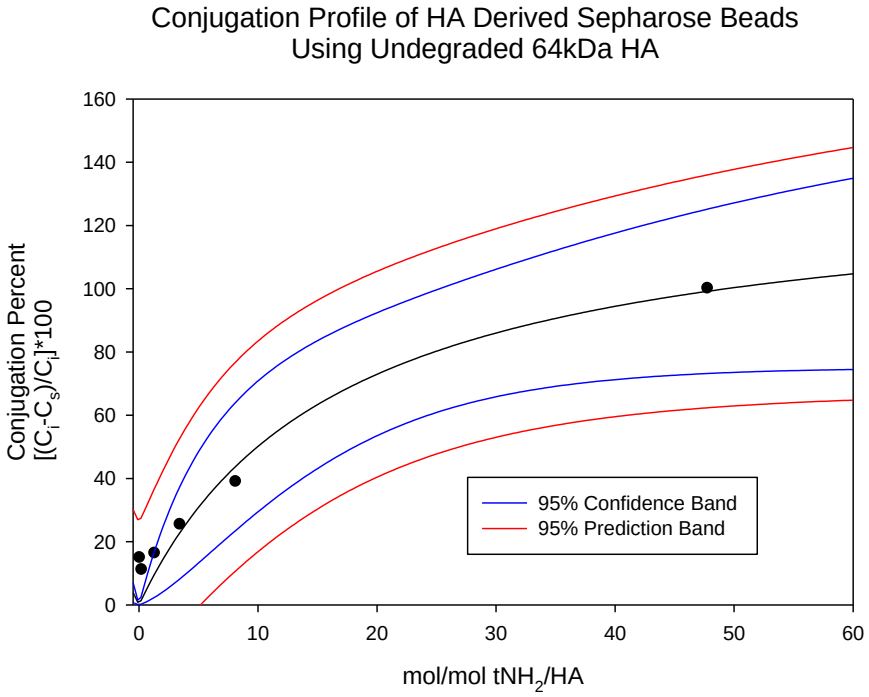

Fig 10: Conjugation percent profile of HA-Sepharose (Affi-gel 102). Red and blue lines bound both a 95% prediction and confidence interval, respectively. Conjugation percent is plotted in terms of the relative molar amounts between the amino groups and HA. R^2=0.9376.

The ratio deduced from the procedure to derive 25ml of equilibrated compact beads with 0.5g 64kDa HA was 48 (Underhill and Zhang). Though HA was treated for 3hr with testicular hyaluronidase (materials and methods), this was an insignificant amount of time to achieve complete degradation (Sakai et. al., 2007). It is therefore assumed HA largely maintained its original MW form.

Plotting the information in terms of percent bead concentration (v/v) per umol HA, the same curve is seen (results not shown). A natural log conversion of this profile was constructed, and linearity fell between a ratio of 2 and 6 (Fig 11).

3.2.2 Fig 11: Natural log conversion of the conjugation profile in terms of bead % (v/v) and umol HA added

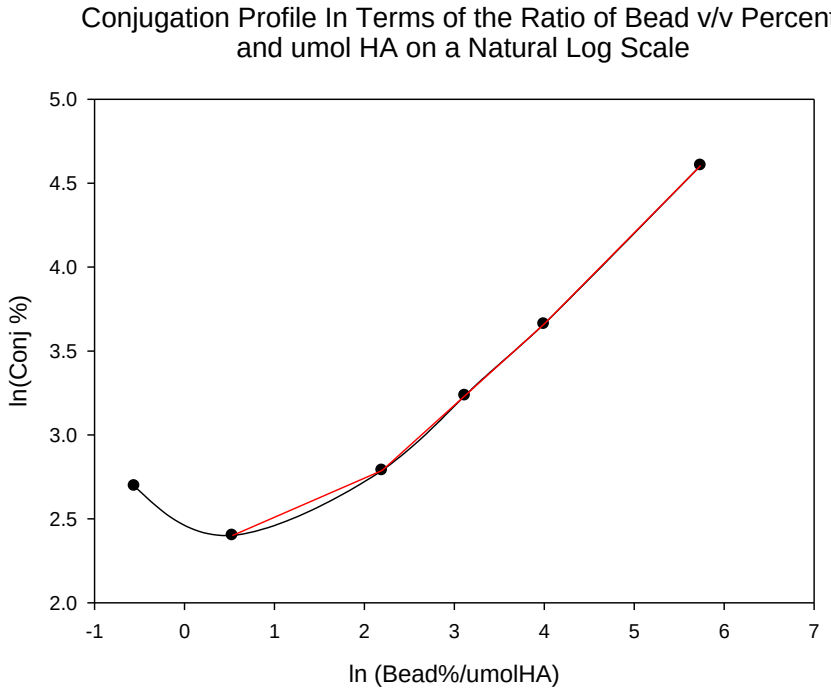

Fig 11: Natural log conversion of the conjugation profile in terms of bead % (v/v) and umol HA added. Results are approximately linear within and including the in (Bead %/umol HA) range of 2 and 6. Black line shows raw results. Red shows results used to deduce a linear relationship.

3.2.3 Fig 12: Plot of natural log conversion profile within selected linear range .

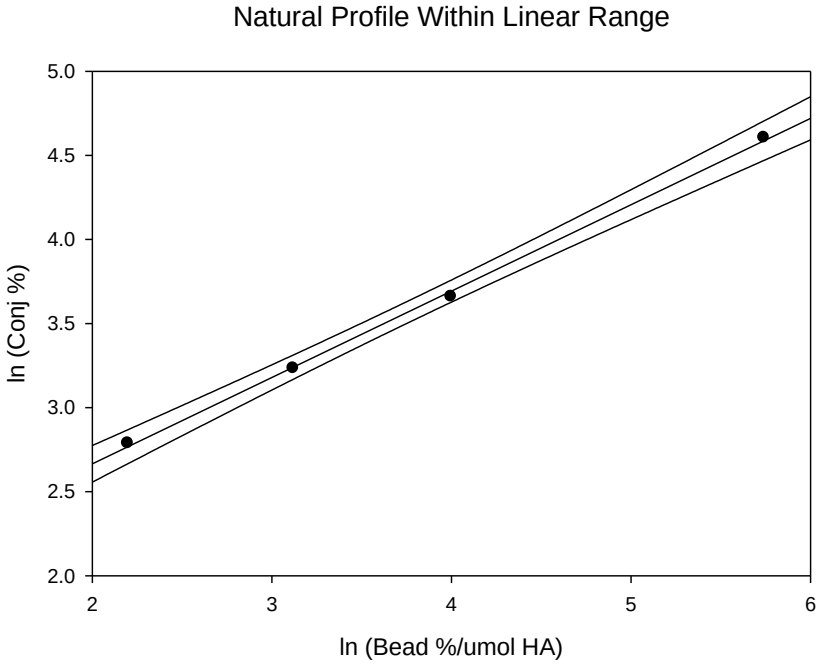

Fig 12: Plot of natural log conversion profile within selected linear range (Fig 11). R^2=0.999, 95% confidence. The corresponding equation used to calculate conjugation percentage came to be: Conj% = 1.6382 (Bead % /umol HA)$^{0.5132}$. The Bead%/umol HA ratio used in the mass incubation was 2.56, giving a conjugation percentage of approximately 3.

Within this range, the results were re-plotted (Fig 12), and the ratio of bead % (v/v) per umol HA was 2.56. The corresponding conjugation value based on this plot was 3 percent. Overall conjugation efficiency would then be the product of two independent factors: mol/mol ratio and bead percent (v/v) = (value attained with Fig 10)*(value attained with Fig 12) = (100%)*(3%) = (100%)*(0.03) =3%. This will be explained more thoroughly in chapter 4.

3.3 HABP Binding Assay

All results for the untrypsinized extract will not be shown, but mentioned as final IMAGE-J analysis from those gels were hard to interpret and resolve. The incubation concentration (IC) prepared in the dilution series of both the UTE and TE were plotted against the total protein coming off in the unbound, 2M NaCl and 4M GCl elution fractions (Fig 13).

3.3.1 Fig 13: Elution plot between the incubation concentration of trypsinized extract and the total protein found between the unbound, and 2M NaCl and 4M GCl elution fractions.

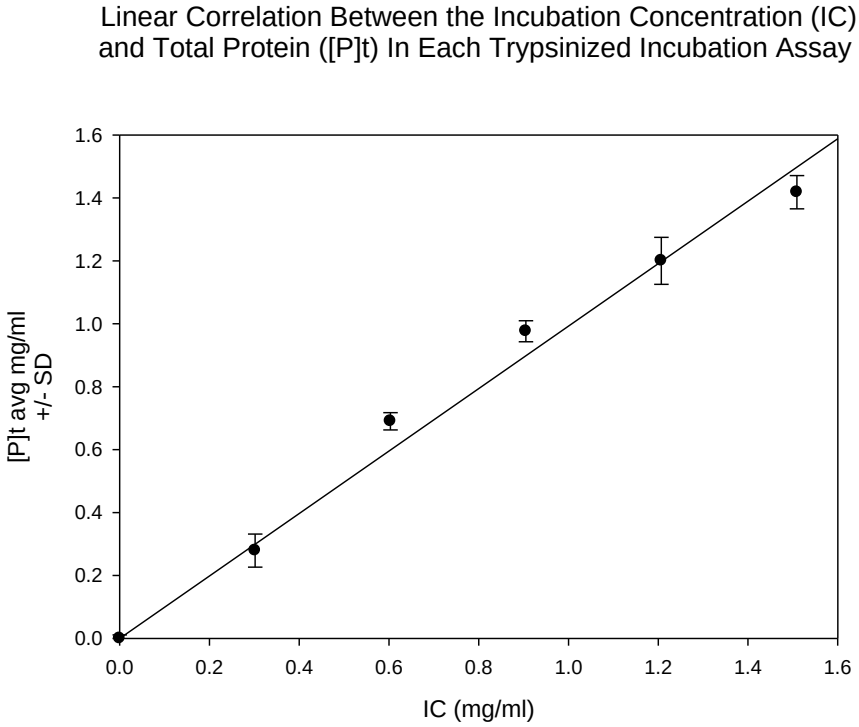

Fig 13: Elution plot between the incubation concentration of trypsinized extract and the total protein found between the unbound, and 2M NaCl and 4M GCl elution fractions. Curve plotted within 95% confidence and is linear after correction to origin ($P<0.001$).

A strong linear correlation was found for both preparations, but only Fig 13 shows the trypsinized results (R^2=0.987 and P<0.001). The corresponding blank measurements (y-intercept) for both the UTE and TE before origin adjustment were 0.0313 mg/ml and 0.0364 mg/ml, respectively. This suggests the used beads themselves did not contribute any significant amount of residual protein that may interfere with the assay. The blank absorbance value calculated from the Bradford standard curve was subtracted from all other measurements which were significantly greater than the blank (P<0.01). A fractional saturation curve was prepared and observed in a Michelis-Menton fashion, and maximum saturation was seen at 0.2855 with a Kd of 0.2460 mg/ml (Fig 14).

3.3.2 Fig 14: Fractional saturation profile of trypsinized extract plotted in terms of the incubation concentration

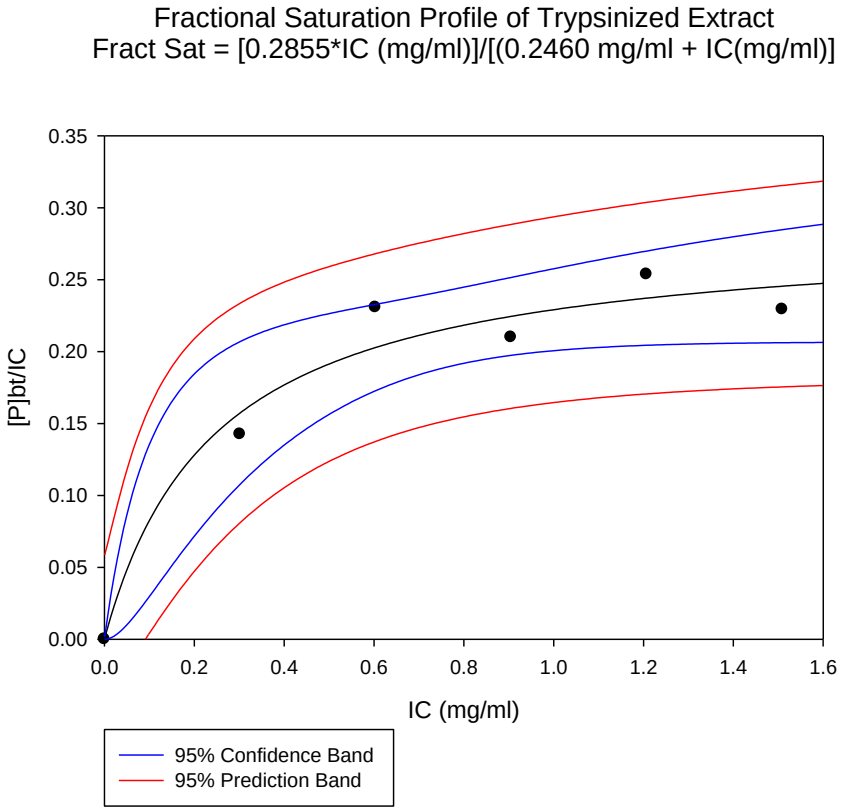

Fig 14: Fractional saturation profile of trypsinized extract plotted in terms of the incubation concentration (IC). Complete fractional saturation reaches its maximum at 0.2855 with a Kd of 0.2460mg/ml. R^2=0.9614.

The fractional values were calculated by dividing the corrected average of the elution fraction by its respective IC. This was mostly contributed by the 2M NaCl elution series as the 4M GCl elution measurements were statistically insignificant from the blank absorbance value. SDS-PAGE was conducted and three bands were analyzed for their ability to bind to the gel (Fig 15, Lane 7, Arrows).

3.3.3 Fig 15: 15% reducing PAGE of 2M NaCl TE elution assay

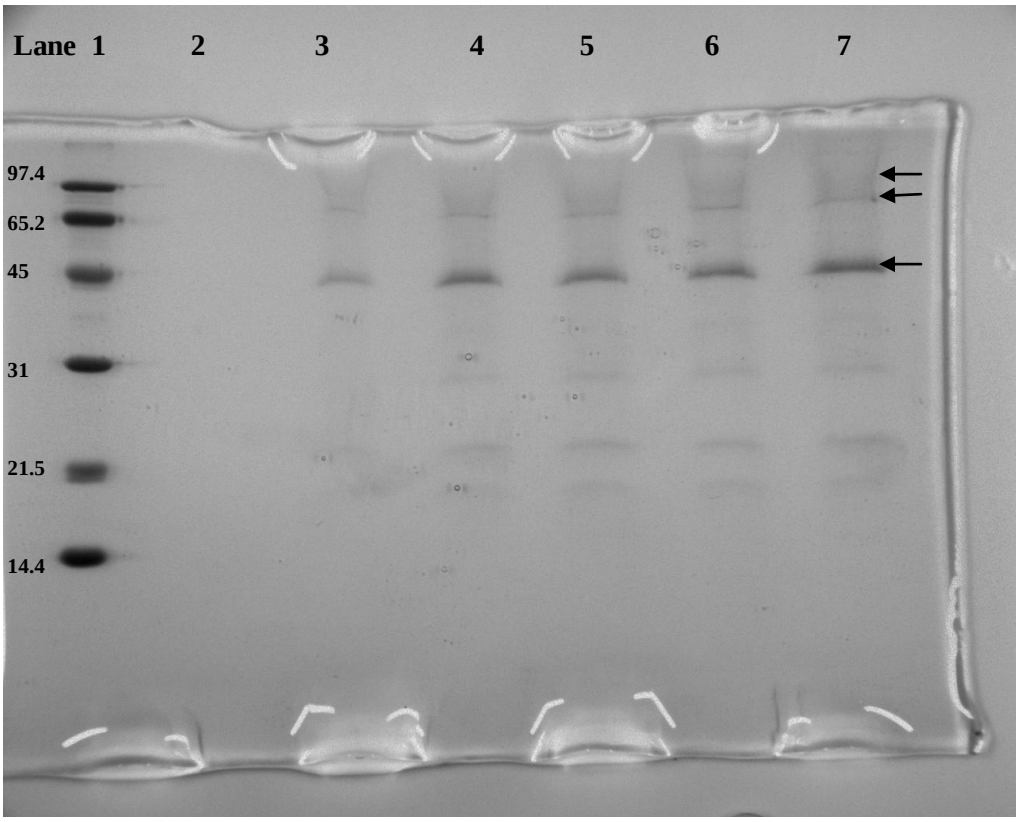

Fig 15: 15% reducing PAGE of 2M NaCl TE elution assay. Lane 1 shows molecular weight marker with corresponding kDa values at left while lanes 2 through 7 show elution results of blank(Lane 2) through 1.509 mg/ml IC (Lane 7). Molecular weight species analyzed shown in Lane 7 at full saturation.

3.3.4 Fig 16: Net intensity profile of 2M NaCl elution at 1.509 IC for the trypsinized extract

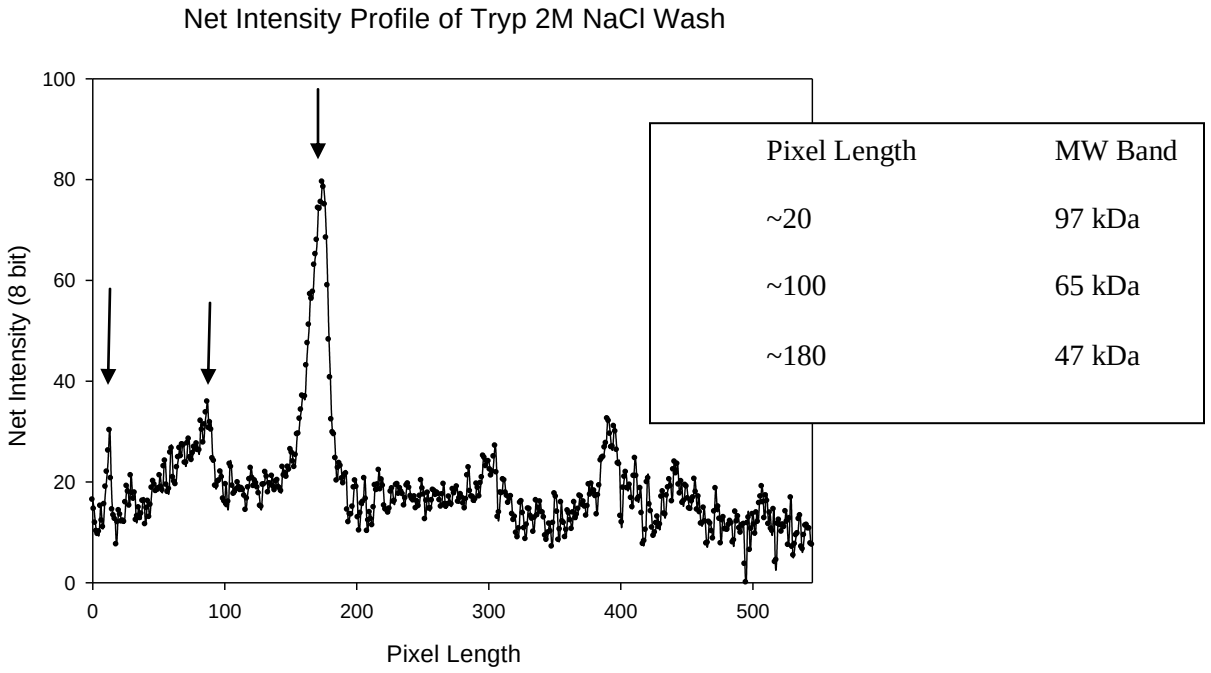

Fig 16: Net intensity profile of 2M NaCl elution at 1.509 IC for the trypsinized extract. The three peaks (arrows) correspond to the molecular weight species analyzed for binding activity: 97kDa, 65kDa and 47kDa. Pixel length is proportional to band migration.

IMAGE-J analysis was performed on the 2M NaCl elution fraction of the 1.509 mg/ml trypsinized incubation (IC) (Fig 15). At this IC, fractional saturation is equal to 0.2455 which is less than 5 percent of the maximum fractional saturation of 0.2855 given by the model (Fig 14). Therefore, maximum saturation can be assumed to be achieved at 1.509 mg/ml IC. This gives a complete assessment of binding capacity for this assay. The net total protein intensity of the individual lane was compared to the net integrated band intensity of the three separate molecular weight species (Fig 16).

Net intensity was calculated using IMAGE-J by subtracting the background gel intensity from the total intensity. All fractional values from the IMAGE-J measurements were calculated as the individual corrected integrated intensity of the band divided by the total corrected intensity of the lane (see materials and methods). The three separate molecular weight species analyzed ran at 97, 65 and 47kDa (Fig 15, Fig 16) giving fractional integrated intensities of 0.006, 0.06 and 0.15, respectively. This gave a total integrated fraction of 0.22 and an intensity ratio of 1:10:25, respectively. The weighted molecular weight average ($\overline{MW}_W$) was calculated to be 53.4 kDa. Since this favors the 47kDa species, its individual contribution was analyzed and shown to be consistent with the overall fractional binding trend (Table 2).

3.3.5 Table 2: Comparison of Average and Specific Binding Fraction of 47kDa Species

1	2	3	4	5	6	7
IC (mg/ml)	Fr. Band Intensity (47 kDa Band)	Protein Binding Fraction +/- SD	Specific Binding Fraction (M)	Specific Binding Fraction x10(-6) M	Average Specific Binding Fraction (M, from $\overline{MW}_w$)	Average Specific Binding Fraction x10(-6) M
0	0	0	0	0	0	0
0.3018	0.1042	0.1425 +/- 2.9826e-3	9.5346x10(-8) M	0.095346	9.52594x10(-8) M	0.0952594
0.6036	0.1455	0.2307 +/- 9.6671e-3	4.3108x10(-7) M	0.43108	3.08440x10(-7) M	0.30844
0.9054	0.1506	0.2099 +/- 0.0183	6.0895x10(-7) M	0.60895	4.20946x10(-7) M	0.420946
1.2072	0.1503	0.2536 +/- 0.0600	9.7902x10(-7) M	0.97902	6.78113x10(-7) M	0.678113
1.509	0.1582	0.2292 +/- 0.0123	1.1642x10(-6) M	1.1642	7.66086x10(-7) M	0.766086

Protein binding fraction: fractional protein content coming off in each elution. This is calculated as [eluted protein amount/IC]. Specific binding fraction: amount of 47kDa species (M) coming off in each fraction. This is calculated as [(Col1)(Col2)(Col3)/47kDa]. Average specific binding fraction: amount analyzed protein coming off in each elution. This is calculated from the weighted molecular weight average [(Col1)(TIF)(Col3)/$\overline{MW}_w$]. TIF=Total Integrated Fraction.

Total binding sites were calculated to be approximately $1.775x10^{-6}$M at maximum saturation, and was derived from both the weighted molecular weight average and the total integrated fraction at full saturation. Kd is defined as the concentration of substrate occupying one-half of the total binding sites, and the corresponding IC value provided by the model is 0.2460mg/ml (Fig 14). With the methods used and the high amount of non-specific binding activity in the crude extract, it is better to interpret substrate binding ability at the point of maximum saturation. So, one-half of the total binding activity {1/2[(0.28)(0.22)]} corresponds to a Kd of $7.235x10^{-8}$M. Though protein levels were insignificant after the 4M GCl elution step, the bands analyzed for binding activity were present to a minimal degree in this series (Fig 17). Interpretation of these results will be explained in the discussion section.

3.3.6 Fig 17: 4M GCl elution assay of trypsinized extract

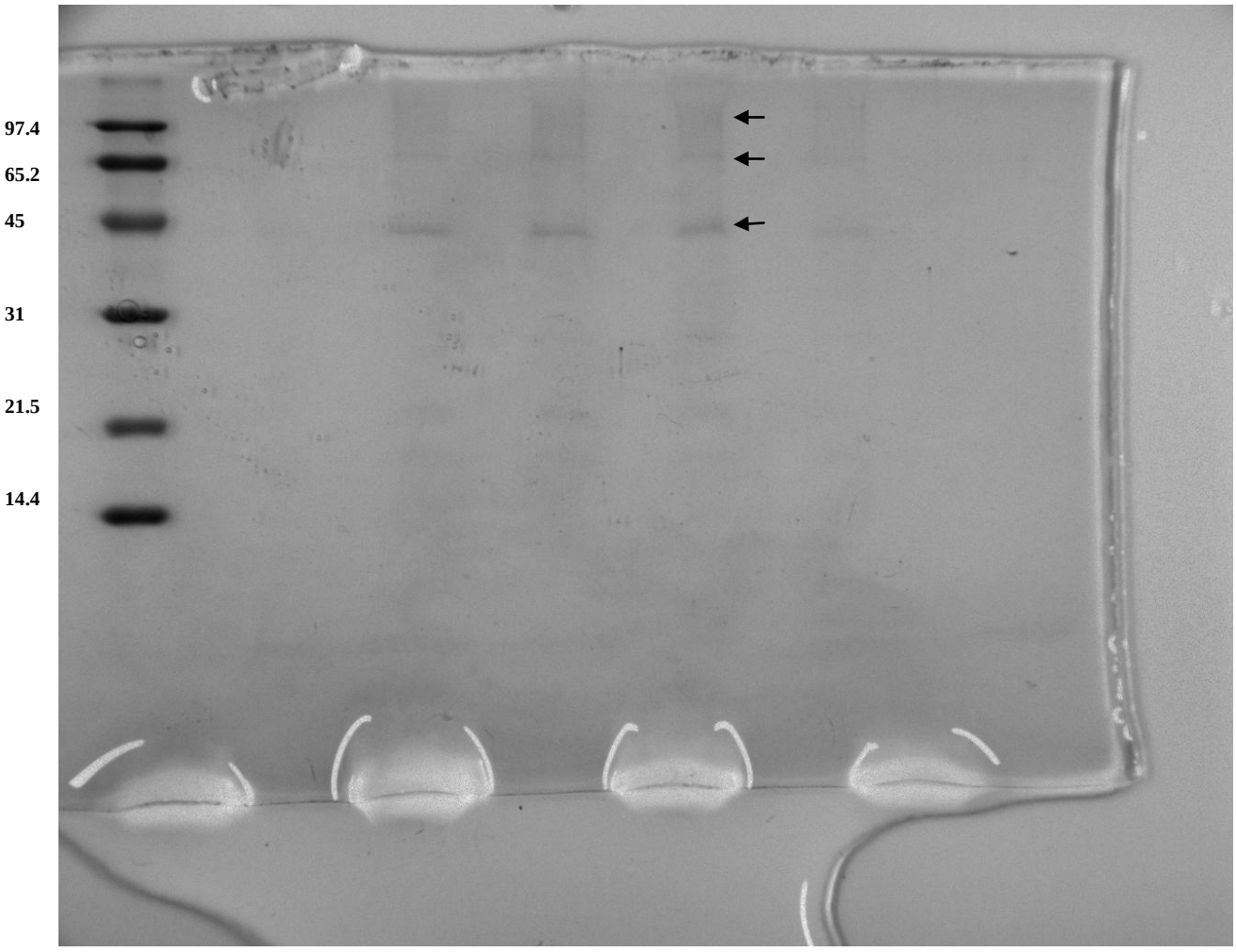

Fig 17: 4M GCl elution assay of trypsinized extract. Lane assignments are consistent with Fig 15. Arrows show the presence of the analyzed molecular weight species in the eluant of the 0.9054 mg/ml trypsinized IC.

3.4 Mass Elution Scheme

With the low binding capacity of the trypsinized extract and the propensity of the derived beads to be largely displaced from the solution if incubated in relatively large volumes, an equal volume ratio of trypsinized extract to derived beads was used in mass extraction and allotted in separate tubes (see materials and methods). An initial elution scheme was devised to follow and approximate the step-wise binding pattern with different molar salt solutions using A280 analysis (Fig 18).

3.4.1 Fig 18: A280 Elution profile of mass elution scheme

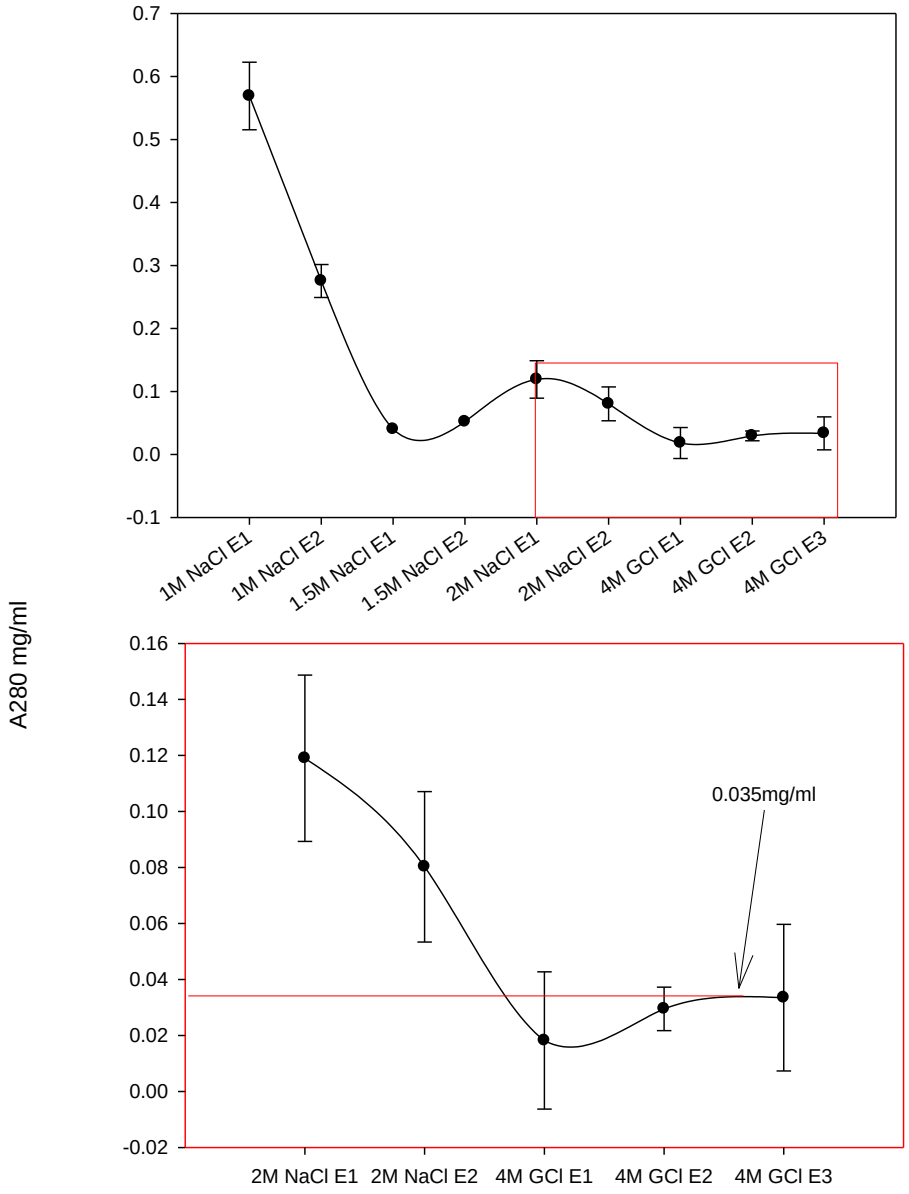

Fig 18. A280 Elution profile of mass elution scheme. Derived and re-stated from Fig 8. Elution steps are labeled on the ordinate with their respective molar salt values. GCl=Guanidinium chloride. Bottom panel shows the highlighted portion in the upper panel on a closer scale. Value of 0.035 mg/ml shows hyperbolic plateau in protein levels through 4M GCl elution series. This corresponds to a 1.18% yield in specific binding activity. Initial extract concentration was 2.9783 mg/ml after blank and Typing/STI correction.

The initial extract concentration after correcting for the blank measurement, STI and Trypsin was 2.9783 mg/ml. Peak binding activity at the 4M GCl elution plateau was 0.035 mg/ml giving a yield of 1.18% in specific binding activity. An initial hump was seen at the first elution volume of 2M NaCl. This may be attributed to proteoglycan HABP subunits having the ability to bind to the derived sepharose beads.

Chapter 4

Conclusion and Discussion

4.1 Putting it All Together

Perhaps the greatest concept taken away from this project and reading material surrounding the basis to isolate and characterize HABPs from bovine nasal cartilage (BNC) is heterogeneity. BNC has to be the perfect tissue to dissect and elucidate the complex inter-relationship of proteoglycans and link-proteins. It is an easy and economical source for this goal, and can be stored for long term use without any significant loss in binding function, though yields are extremely low.

BNC is a highly tensile tissue, and its physiological function structurally initiates proper laminar airflow to the lungs. Inhaling through the nose and exhaling out the mouth is a simple example of breathing efficiency. The turbulence resulting from the large amount of air coming in through the oral cavity decreases the potential for oxygen to reach the caudal part of the lungs where the surface area to volume ratio of dense alveolar tissue is maximal. Nasal septa can be thought of as a pillar to support the intake conduit to the trachea for directing smooth airflow, thus resulting in maximum breathing efficiency and hemoglobin saturation. Glycoprotein and GAG polymers cohesively interact with collagen to produce its characteristic mechanical behavior seen in cartilage.

Targeting the extraction and isolation of HABPs from this tissue requires aggressive steps to realize a practical yield of viable protein. This project was primed by previous work in isolating the HA binding fraction of BNC using conventional liquid chromatographic methods (Tengblad, 1978).

In this case, the binding yield was 2.5%, and 4M GCl was specifically administered as the reversible denaturant to rinse off, collect and measure HABPs from HA-derived sepharose beads.

The yield using the current mass incubation scheme with trypsinized extract deduced from the defined Micheles-Menton elution plateau with three successive volumes of 4M GCl was calculated to be 1.18% (Fig 18, Lower Panel). Due to the large loss of binding activity after 2M NaCl elution in the HABP binding assay, this scheme was devised to follow total protein coming off the HA-derived beads through a step-wise increase in ionic strength. Successive equal-volume washes from 1M to 1.5M NaCl E1 (first elution volume) initially showed a precipitous decline in binding activity. This may be non-specific material coming off the beads such as collagen, and C-terminal proteoglycan fragments left-over after BNC solubilization and trypsinization. As the ionic strength is pushed up to 2M NaCl E2 (second elution volume), a hump is observed (Fig 18, upper panel). At this stage, N-terminal HABP binding substituents of proteoglycan trypsinized monomers are most likely being eluted. Keratin sulfate and chondroitin sulfate GAG substitution along the protein core near the HABP binding domain is causing the protein to spread out and interact more appreciably with the high molar NaCl content.

DEAE column fractions of BNC tryptic fragments with high buoyant density have been shown to express a relatively high amount of Ser content, a favorable ratio between Cys and BAARs to compose the binding domain, increased ionic selectivity upon elution and co-immunoprecipitation against anti-bodies selective for proteoglycan fractions that were digested with both chondroitinase and hyaluronidase. (Keiser et.al., 1971; Keiser and Hatcher, 1977; Keiser, 1982; Keiser et.al., 1982). The high amount of non-specific material being excluded early in the mass-elution scheme is consistent with binding saturation experiments using Sephadex-G200 chromatography where the reactive proteoglycan complex is shifted to the void volume, and a large amount of the remaining protein is contained in a fraction at the low end of the elution range (Heinegaard and Hascall, 1974).

Buoyant density differences between PG HABP monomers and smaller more specific HABPs in BNC have been shown using a procedure to label the aggregated A1 fraction (Heinegaard and Hascall, 1974). PG monomers are found at the bottom of a dissociative CsCl equilibrium gradient, but run at a high molecular weight in an SDS reducing PAGE stained with Coomassie blue. The spreading pattern is imposed by Ser O-glycosylation of chondroitin and keratin sulfate making the band appear diffuse in the gel. This increases the surface area of the PG monomer which may be limiting its migration through the polyacrylamide gel. The monomer's inherent density enables it to spin down to the higher end of the CsCl gradient. Together, GAG substitution and its interaction with the PG monomer HA-binding domain regulate its association with the aggregated A1 complex, and leads to the manipulation of solvent conditions to select for specific binding activity. This will be explained in more detail later.

The A1 fraction is composed of the functional binding complex known as aggrecan, and can be separated in an associative CsCl gradient with crude extract. The unifying substituent to mediate aggregation between proteoglycan monomers and link proteins is hyaluronic acid. Separation procedures prior to the work by Tengblad have used different solvent conditions in order to solubilize functional binding fractions, also known as "link" fractions. Cartilage tissue has been treated with KCl, $MgCl_2$, GCl and $CaCl_2$. 4M GCl has been found to produce the maximal concentration of solubilized hexauronate (Sajdera and Hascall, 1969), and this project re-affirmed this procedure with the 30hr incubation of grated cartilage tissue in the same solvent (Fig 3) GCl has the ability to decrease the T_m of protein at high concentrations while stabilizing or even enhancing it at lower concentrations (Mayer and Schmid, 1993). The loss in Gibb's free energy of HABPs after dialyzing the extract in proper solution conditions can be comparable to reclaiming a native state. GCl is a reversible denaturant allowing dissociation and reconditioning of native complexes.

The non-Newtonian behavior of the proteoglycan A1 aggregate ascribes its high sedimentation value and concentration-dependent viscosity, and can be appreciated by sedimentation experiments. The functional aggregated complex seems to be separated more efficiently using 4M GCl opposed to 3M $MgCl_2$. The sedimentation profiles of the extract are universally bi-modal, but when 3M $MgCl_2$ is used as the extracting solvent, most of the hexauronate spins down in the faster sedimenting mode (Sajdera and Hascall, 1969). Protein yield and amino acid content between these two solution conditions are relatively similar. The faster mode seen with the 4M GCl extract is the functional A1 complex, and represents roughly twenty percent of total equilibrated content. When the solution is reduced with dithiothreitol, it shifts to the lower modal value and loses its aggregation potential (Sajdera and Hascall, 1969). This chemically modified PPC represents less than eight percent protein which is consistent with low yields of the link fraction.. Cysteine is a necessary amino-acid to maintain the proper three-dimensional fold of the HABP binding domain, and when it is reduced those bridges collapse resulting in the protein to lose its integrity and drag in solution. Other experiments show that modifying amino groups of HABP extracts lose a significant amount of binding activity (Heinegaard and Hascall, 1979). Similar results using trypsinized binding fragments to saturate added amounts of HA and collecting those functional binding complexes in the excluded volume of Sephardic G200 columns show a relatively large amount of non-specific protein eluting in the total volume of the chromatogram, discussed earlier (Heinegaard and Hascall, 1974). Roughly thirty percent of the total protein was identified as both the PG HABP monomers (90 kDa species) and the more specific link protein (45kDa). From the results given by Heinegaard and Hascall, the specific yield contribution by both species is inferred to be 14% and 5%, respectively.

This proportion agrees with the current project where maximum binding saturation of the trypsinized extract was found at a total fraction of twenty-nine percent, the maximum value of the PG monomer hump is five-percent and the value corresponding to specific binding activity is 1.18%. These low values engender the need of affinity column chromatography to exclude non-specific remnants from the original tissue source.

After this sample was prepared, several biochemical measurements were made. A spectromatogram was analyzed through the full UV range and found to be dirty. However, both BCA and A280 measurements agreed well with a purchased stock preparation of lyophilized HABPs. Using more specific methods to isolate native binding activity such as a western blot with labeled HA-FITC, or competitive binding assays will help define a workable concentration for preparing potent in-vivo injections.

The prominent bands analyzed ran at 97kDa, 64kDa and 47kDa. Three species were chosen, because a possible discrepancy in the results by Tengblad show binding ability of a 68kDa and 45kDa species, but discuss the 90kDa species in place of the former. Other reports suggest and show the presence of both the 90kDa HABP PG monomer and 45kDa link protein (Tengblad, 1978; Heinegaard and Hascall, 1974). For these reasons the 97, 65 and 47kDa species were analyzed. The 47kDa species is proposed to be the link protein, with a sixteen-percent specific binding fraction determined by Image-J analysis (Table 2). Reports using frontal gel chromatography show twenty-percent specific binding activity, and this low amount was justified by both the different binding capabilities of link proteins within the complex and variable heterogeneity of intact BNC (Lyon and Nieduszynski, 1983).

The way in which this project was conducted was a crude attempt at isolating viable protein within the trypsinized extract having the inherent ability to bind to HA-derived sepharose beads. For this reason, a pull down incubation method was used.

The initial HABP binding assay was essentially conducted in a two step process in order to characterize binding ability and differential yield. After the beads were incubated overnight in associative conditions, 2M NaCl then 4M GCl solvents were used to wash off protein remaining on the surfaces of the beads. As discussed in the results section, there was an insignificant amount of protein that retained its ability to bind to the beads when 4M GCl was used. This is also shown in Fig 17. At high ICs, a decline in protein elution is observed. Proteoglycans, by their nature, have the ability to self aggregate and this can be seen in Schleridien patterns and centrifugation analysis (Sajdera and Hascall, 1969; Hascall and Heinegaard, 1974; Hascall and Sajdera, 1969). Though the functional binding complex is retained in the A1 fraction after associative CsCl centrifugation, much of the PG constituents are mixed in this complex and may have interfered with the targeted protein's ability to bind to its substrate. An associative CsCl gradient was not used in this project, so the harvested solution contained all known constituents when pull-down incubation was initiated. As the IC reached it threshold, the PG monomers may have induced non-specific aggregation with HABPs in the extract causing a significant amount of protein to be washed off with 2M NaCl. This can be more appreciated in the mass elution scheme (Fig 18).

The hump observed as the ionic strength gradually increases from 1M NaCl to 2M NaCl before reaching the more specific elution volumes of 4M NaCl is most likely the PG HABP monomers washing off from HA. The glycosylated GAG groups covalently attached to Ser residues in these monomers may be destabilizing the thermodynamic requirement ("spreading" phenomenon) to remain attached. This is highlighted by the abrupt decline in A280 at the second elution volume of 2M NaCl (2M NaCl E2). Therefore, the low yield calculated by extrapolating the value corresponding to the level of the Micheles-Menton plateau from successive 4M GCl elutions should be partially explained by heterotypic interaction of PG HABP monomers. It can also be due to the low conjugation percentage of HA-Sepharose derivitization.

Conjugation depended on both the relative concentrations between amino-derived beads and HA, and HA MW. It was expressed in the introduction that the concentration and molecular weight of HA in solution affects its surface-area presentation deduced by NMR spectroscopy. This would lead to a deviation in its conjugation ability. IR spectra have been used to delineate the absorbance differences between chondroitin sulfate and hyaluronic acid in terms of relative hydration percentage (Servatty et. al, 2001). An additional experiment was conducted to confirm this observation by controlling for high absorbance values seen at the low UV range in a diluting mixture of 64 kDa HA with albumin. The same shifting behavior in the absorbance peak of HA at relative dilution values was seen, but needs to be re-assessed. Hyaluronic acid's hygroscopic nature and its ability to "open up" as the solution becomes more dilute gives a higher probability for conjugation with increasing MW HA derivatives. This can be observed with increasing solution viscosity as the concentration of HA increases. It would also provide a suitable explanation that a 2.4% (w/v) limit was achieved with 64kDa HA when preparing the stock solution, and would agree with other reports (Yanaki and Yamaguchi, 1990) The limitation of HA conjugation with amino-derived sepharose beads was calculated at a low three-percent, and can only be due to high molecular weight and the relative concentration factor between HA and sepharose beads. The conjugation reaction is entropically-driven and the independent contribution of these two factors weigh in the overall calculation of conjugation percentage. This needs to be followed up by more specific methods to define HA MW, and its role in conjugation efficiency.

Colorimetric procedures have been used to quantify HA MW in solution, and is directly proportional to the reducing-end amount (Asteriou et.al., 2001) The time for HA degradation prescribed for bead conjugation was three hours, and twelve hrs is needed to see a significant decline in MW thus preventing autonomous HA association and tertiary aggregate formation.

A more suitable time-frame can be found to attain the optimal HA size in order to achieve a definite maximum in conjugation leading to more reliable increases in specific binding yields.

4.2 Interpreting the Calculations: Binding Values and Saccharide Dependency

Eluted band intensities were carried over in a proportional fashion running at 65kDa in the UTE 4M GCl elution assay (results not shown). This may represent untrypsinized material having the ability to bind to HA, and controls for the validity of the binding assay itself. Since these results overlap that of the TE, it also may provide proof of heterotypic interference by trypsinzed PG monomers. Using the calculated $\overline{MW}_w$ and SigmaPlot curve-fitting program, the concentration of total binding sites ([TBS]) and Kd of trypsinized HABPs is $1.775x10^{-6}$M and $7.235x10^{-8}$M, respectively. Scatchard analysis cannot be generated due to the inability of molecular weight binding contributions to be resolved at the low end of the incubation assay, and the exceptional amount of non-specific binding activity.

The average specific binding fraction of the 47kDa binding species was calculated to be $0.766x10^{-6}$M at 1.509mg/ml IC (Table 2) showing most of the activity to be favor the link protein. The molar content of HABPs between PG monomers and link proteins are essentially the same at full saturation, but the amount of added HA needed to reach this point was 7.5x higher with link proteins (Heinegaard and Hascall, 1974). The size of HA used in this report was 230kDa giving 583.3 disaccharide units, where the molecular weight of one glucuronic acid-glucosamine unit is 394.3 g/mol. Link proteins were able to cover an average of 45 units, though differences have been reported (Lyon and Niedusynski, 1983). There have been reports of temperature affecting affinity (Lyon and Niedusynski, 1983), but conditions were kept constantly cold in the current project except where measurements were being made. Together with reliable data, this ensures a viable sample was prepared post mass preparation.

Nevertheless, when trying to enhance the purity of the sample and provide a good amount of HABPs from BNC, traditional liquid affinity chromatography needs to be used in conjunction with western-blot and ligand binding assays. Having all the amenable resources necessary to achieve this end are more than welcome. This will establish a suitable starting point for in-vivo preparation and analysis.

4.3 Statistical Methods

All measures of significance between the mean values of eluted protein and refractive indices of post-conjugated supernatant, and their respective blank measurements were conducted with the Minitab computer program (Student Version 14) using the student's t-test. Curve-fitting and plot generation was done using Sigmaplot v10.0, which enabled statistical analysis and interpretation.

References

Adamson, R.H. Permeability of frog mesenteric capillaries after partial pronase digestion of the endothelial glycocalyx. *Journal of Physiology*. **428**, 1-13, 1990.

Antonopoulous, C.A. et.al. Extraction and purification of proteoglycans from various types of connective tissue. *Biochimica et Biophysica Acta*. **338**, 108-119, 1974

Asteriou, T. et.al. An improved assay for the N-acetyl-D=glucosamine reducing ends of the polysaccharides in the presence of proteins. *Analytical Biochemistry*. **293**, 53-59, 2001.

Asteriou, T. et.al. Inhibition of hyaluronan hydrolysis catalyzed by hyaluronidase at high substrate concentrations and low ionic strength. *Matrix Biology*. **25**, 166-174, 2006.

Balazs, E.A. et. al. Transient intermediates in the radiolysis of hyaluronic acid. *Radiation Research*. **31**, 243-255, 1967.

Bartolazzi, A. et.al. Regulation of growth and dissemination of a human lymphoma by CD44 splice variants. *Journal of Cell Science*. **108**, 1723-1733, 1995.

Bergqvist, Ann-Sofi et.al. Hyaluronan and its binding proteins in the epithelium and the intraluminal fluid of the bovine oviduct. *Zygote*. **13**, 207-218, 2005.

Bignami, A., Hosley, M. and Dahl, D. Hyaluronic acid and hyaluronic acid-binding proteins in brain extracellular matrix. *Anat. Embryol.* **188**, 419-433, 1993.

Bourguignon, L.Y.W. et.al. Rho-kinase (ROK) promotes $CD44_{3, 8-10}$-ankyrin interaction and tumor cell migration in metastatic breast cancer cells. *Cell Motility and the Cytoskeleton.* **43**, 269-287, 1999.

Brightman, M.W. and Kaya, M. Permeable endothelium and the interstitial space of brain. *Cellular and Molecular Neurobiology.* **20**(2), 111-130, 2000.

Cohen, M. et.al. Organization and adhesive properties of the hyaluronan pericellular coat of chondrocytes and epithelial cells. *Biophysical Journal*. **85**, 1996-2005,2003.

Culty, M. et.al. The hyaluronate receptor is a member of the CD44 (H-CAM) family of cell surface glycoproteins. *The Journal of Cell Biology.* **111**(6,Part 1), 2765-2774, 1990.

Day, A.J. et.al. Overexpression, purification and refolding of link module from human TSG-6 in *Escherichia coli*: effect of temperature, media and mutagenesis on lysine misincorporation at arginine AGA codons. *Protein Expression and Purification.* **8**, 1-16, 1996.

Doege, K. et.al. Link protein cDNA sequence reveals a tandemly repeated protein structure. *Proc. Natl. Acad. Sci.* **83**, 3761-3765, 1986.

Engstrom-Laurent, A. and Hallgren, R. Circulating hyaluronic acid levels vary with physical activity in healthy subjects and in rheumatoid arthritis patients. *Arthritis and Rheumatism*. **30**(12), 1333-1338, 1987.

Estess, P. et.al. Interleukin 15 induces endothelial hyaluronan expression in-vitro and promotes activated T cell extravasation through a CD44-dependent pathway in-vivo. *J. Exp. Med*. **190**(1), 9-19, 1999.

Fraser, J.R.E., Laurent, T.C. and Laurent, U.B.C. Hyaluronan: its nature, distribution, functions and turnover. *Journal of Internal Medicine.* **242**, 27-33, 1997.

Genasetti, A. et.al. Hyaluronan and human endothelial cell behavior. *Connective Tissue Research*. **49**, 120-123, 2008.

Gerdin, B. and Hallgren, R. Dynamic role of hyaluronan (HYA) in connective tissue activation and inflammation. *Journal of Internal Medicine.* **242**, 49-55, 1997.

Goetinck, P.F. et. al. The tandemly repeated sequences of cartilage link protein contain the sites for interaction with hyaluronic acid. *The Journal of Cell Biology.* **105**, 2403-2408, 1987.

Goldstein, L.A. et.al. A human lymphocyte homing receptor, the hermes antigen, is related to cartilage proteoglycan core and link proteins. *Cell.* **56**, 1063-1072, 1989.

Goueffie, Y. et.al. Hyaluronan induces vascular smooth muscle cell migration through RHAMM-mediated PI3K-dependent Rac-activation. *Cardiovascular Research.* **72**, 339-348, 2006.

Gouverneur, M. et al. Fluid shear stress stimulates incorporation of hyaluronan into endothelial cell glycocalyx. *Am J Heart Circ Physiol*. **290**, H458-H462, 2006.

Greenwald, R.A. Oxygen radicals, inflammation, and arthritis: pathophysiological considerations and implications for treatment. *Seminars in Arthritis and Rheumatism.* **20**(4), 219-240, 1991.

Gregory, J.D. Short communication: multiple aggregation factors in cartilage proteoglycan. *Biochem. J.* **133**, 383-386, 1973

Hascall, V.C. and Heinegaard, D. Aggregation of cartilage proteoglycans I. The role of hyaluronic acid. *The Journal of Biological Chemistry*, **249**(13), 4232-4241, 1974

Hascall, V.C. and Sajdera, S.W. Proteinpolysaccharide complex from bovine nasal cartilage: the function of glycoprotein in the formation of aggregates. *The Journal of Biological Chemistry*. **244**(9), 2384-2396, 1969.

Hascall, V.C., and Heinegaard, D. Aggregation of cartilage proteoglycans II. Oligosaccharide competitors of the proteoglycan hyaluronic acid interaction. *The Journal of Biological Chemistry*.**249**(13), 4242-4249, 1974.

Heinegaard, D. Extraction, fractionation and characterization of proteoglycans from bovine tracheal cartilage. *Biochimica et Biophysica Acta*. 181-192, 1972.

Heinegaard, D. and Hascall, V.C. Aggregation of cartilage proteoglycans III. Characteristics of the proteins isolated from trypsin digests of aggregates. *The Journal of Biological Chemistry.* **249**(13), 4250-4256, 1974.

Heinegaard, D.B. and Hascall, V.C. The effects of dansylation and acetylation on the interaction between hyaluronic acid and the hyaluronic acid binding region of cartilage proteoglycans. *The Journal of Biological Chemistry.* **254**(3), 921-926, 1979,

Heldin. P., Laurent, T.C. and Heldin, C.H. Effect of growth factors on hyaluronan synthesis in cultrured human fibroblasts. *Biochem. J.* **258**, 919-922, 1989.

Henry, C.B.S. and Duling, B.R. Permeation of the luminal capillary glycocalyx is determined by hyaluronan. *The American Physiological Society. H508-H514, 1999.*

Hoffman, P. Selective aggregation of proteoglycans with Hyaluronic Acid. *The Journal of Biological Chemistry.* **254**(23), 11854-11860, 1978.

Kawahara, K. and Tanford, C. Viscosity and density of aqueous solutions of urea and guanidine hydrochloride. *Journal of Biological Chemistry.* **241**(13), 3228-3232, 1966.

Keiser, H.D. Immunodiffusion studies of the tryptic fragments of bovine nasal-cartilage proteoglycan monomer of high buoyant density. *Biochem. J.* **203**, 691-698, 1982.

Keiser, H.D. and Hatcher, V.B. A comparison of bovine nasal cartilage proteoglycan core protein produced by chondroitinase and hyaluronidase: the possible role of protease contaminants. *Connective Tissue Research.* **5**, 147-155, 1977.

Keiser, H.D., Adlersberg, J.B. and Steinman, H.M. Isolation and biochemical characterization of the tryptic fragments of bovine nasal-cartilage proteoglycan monomer of high buoyant density. *Biochem. J.* **203**, 683-689, 1982.

Keiser, H.D., Shulman, H.J., and Sandson, J.I. Immunochemistry of cartilage proteoglycan. *Biochem. J.* **126**, 163-169, 1972.

Kohda, D. et.al. Solution structure of the link module: a hyaluronan-binding domain involved in extracellular matrix stability and cell migration. *Cell.* **86**, 767-776, 1996.

Lark, M.W. Aggrecan Degradation in Human Cartilage: Evidence for both Matrix Metalloproteinase and Aggrecanase Activity in Normal, Osteoarthritic, and Rheumatoid Joints. *J. Clin. Invest.* **100**(1), 93-106, 1997.

Laurent, T.C. and Fraser, R.E. Hyaluronan. *The FASEB Journal.* **6**, 2397-2404, 1992

Lesley, J., Schulte, R. and Hyman, R. Binding of hyaluronic acid to lymphoid cell lines is inhibitied by monoclonal antibodies against Pgp-1. *Experimental Cell Research.* **187**, 224-233, 1990.

Lesley, T. et.al. Hyaluronan binding function of CD44 is transiently activated on T cells during an in-vivo immune response. *J. Exp. Med.* **180**, 383-387, 1994.

Liu, N. et.al. Metastatin: a hyaluronan-binding complex from cartilage that inhibits tumor growth. *Cancer Research.* **61**, 1022-1028, 2001.

Luscombe, M. and Phelps, C.F. Action of degradative enzymes on the light fraction of bovine septa protein polysaccharide. *Biochem. J.* **103**, 103-109, 1967

Luscombe, M. and Phelps, C.F. The composition and physiochemical properties of bovine nasal-septa protein-polysaccharide complex. *Biochem. J.* **102**, 110-118, 1967

Lyon, M. and Nieduszynski, I.A. A study of equilibrium binding of link protein to hyaluronate. *Biochem. J.* **213**, 445-450, 1983

Mayr, L.M. and Schmid, F.X. Stabilization of a protein by guanidinium chloride. *Biochemistry.* **32**, 7994-7998, 1993.

Melrose, J., Numata, Y. and Ghosh, P. Biotinylated hyaluronan: a versatile and highly sensitive probe capable of detecting nanogram levels of hyaluronan binding proteins (hyaladherins) on electroblots by a novel affinity detection procedure. *Electrophoresis.* **17**, 205-212, 1996.

Mochizuki, S. et. al. Role of hyaluronic acid glycoaminoglycans in shear-induced endothelium-derived nitric oxide release. *Am J Physiol Heart Circ Physiol.* **285**, H722-H726, 2003.

Ohno, H. et.al. Calibration of the relative molecular mass of proteoglycan subunit by column chromatography on Sepharose CL-2B. *Biochem. J.* **235**, 553-557, 1986.

Oliferenko, S. et.al. Hyaluronic acid (HA) binding to CD44 activates Rac1 and induces lamellipodia outgrowth. *The Journal of Cell Biology*. **148**(6), 1159-1164, 2000.

Pahakis, M.Y. et.al. The role of endothelial glycocalyx components in mechanotransduction of fluid shear stress. *Biochem. Biophys. Res. Commun.* **355**(1), 228-233, 2007.

Pal, S., Doganges, P.T. and Schubert, M. The separation of new forms of the proteinpolysaccharides of bovine nasal cartilage. *The Journal of Biological Chemistry*, **241**(18), 4261-4266, 1966

Perlin, J.P. et. al. Structural data concerning the link proteins from bovine nasal cartilage proteoglycan complex. *FEBS Letters*, **119**(2), 333-336, 1980.

Reitsma, S., Staaf, D.W. and Vink, H. The endothelial glycocalyx: composition, functions, and visualization. *Eur J Physiol*. **454**, 345-359, 2007.

Roscic-Mrkic, B. et.al. RANTES (CCL5) uses the proteoglycan CD44 as an auxiliary receptor to mediate cellular activation signals and HIV-1 enhancement. *Chemokines*, **102**(4), 1169-1177, 2003.

Rosenberg, L. and Schubert, M. The proteinpolysaccharides of cartilage. *Rheumatology.* **3**, 1-60, 1970.

Rosenberg, L., Hellman, W., and Kleinschmidt, A.K. Molecular models of proteinpolysaccharides from bovine nasal cartilage based on electron microscopic studies. *The Journal of Biological Chemistry.* **245**(16), 4123-4130, 1970.

Rosenberg, L., Pal. S., Beale, R., and Schubert, M. A comparison of proteinpolysaccharides of bovine nasal cartilage isolated and fractionated by different methods. *The Journal of Biological Chemistry.* **245**(16), 4112-4122, 1970.

Sajdera, S.W. and Hascall, V.C. Proteinpolysaccharide complex from bovine nasal cartilage: a comparison of low and high shear extraction procedures. *The Journal of Biological Chemistry*, **244**(1), 77-87, 1969

Sakai, S. et. al. Matrix assisted laser desorption ionization-time of flight mass spectrometry analysis of hyarluronan oligosaccharides. *Analytica Chimica Acta.* **593**, 207-213, 2007.

Scott, J. and Heatley, F. Hyaluronan forms specific stable tertiary structures in aqueous solution: A ^{13}C NMR study. *Proc. Natl. Acad. Sci.* **96,** 4850-4855, 1999.

Servaty, R. et.al. Hydration of polymeric components of cartilage-an infrared spectroscopic study on hyaluronic acid and chondroitin sulfate. *International Journal of Biological Macromolecules.* **28**, 121-127, 2001.

Siegelman, M.H., DeGrendele, H.C. and Estess, P. Activation and interaction of CD44 and hyaluronan in immunological systems. *Journal of Leukocyte Biology***. 66**, 315-321, 1999.

Singleton, P.A. and Bourgulgnon, L.Y.W. CD44v10 interaction with Rho-kinase (ROK) activates inositol 1,4,5-triphosphate (IP_3) receptor mediated Ca^{2+} signaling during hyaluronan (HA)-induced endothelial cell migration. *Cell Motility and the Cytoskeleton.* **83,** 293-316, 2002.

Smith, J.W., Peters, T.J. and Serafini-Fracassini, A. Observations on the distribution of the proteinpolysaccharide complex and collagen in bovine articular cartilage. *J. Cell. Sci.* **2**, 129-136, 1967.

Speziale, P. et.al. Interactions between different corneal proteoglycans. *Biochem J.* **173**, 935-939, 1978

Squire, J.M. et.al. Quasi-periodic substructure in the microvessel endothelial glycocalyx: a possible explanation for molecular filtering? *Journal of Structural Biology.* **136**, 239-255, 2001.

Stamenkovic, I. et.al. The hematopoietic and epithelial forms of CD44 are distinct polypeptides with different adhesion potentials for hyaluronate-bearing cells. *The EMBO Journal.* **10**(2), 343-348, 1991.

Stamenkovic, I. et.al. A lymphocyte molecule implicated in lymph node homin is a member of the cartilage link protein family. *Cell.* **56**, 1057-1062, 1989.

Stern, R., Asari, A.A. and Sugahara, K.N. Hyaluronan fragments: an information –rich system. *European Journal of Cell Biology.* **85**, 699-715, 2006.

Tabata, T. et.al. Low molecular weight hyaluronan increases the uptaking of oxidized LDL into monocytes. *Endocrine Journal*. **54**(5), 685-693, 2007.

Taylor, K.R. et. al. Hyaluronan fragments stimulate endothelial recognition of injury through TLR 4. *The Journal of Biological Chemistry*. **279**(17), 17079-17084, 2004.

Tengblad, A. A comparative study of the binding of cartilage link protein and the hyaluronate-binding region of the cartilage proteoglycan to hyaluronate-substituted Sepharose gel. *Biochem. J.* **199**, 297-305, 1981.

Tengblad, A. Affinity chromatography on immobilized hyaluronate and its application to the isolation of hyaluronate binding proteins from cartilage. *Biochimca et Biophysica Acta*, **578**, 281-289, 1979

Termeer, C. et.al. Oligosaccharides of hyaluronan activate dendritic cells via toll-like receptor 4. *J. Exp. Med.* **195**(1), 99-111, 2002.

Toole, B.P. Hyaluronan and its binding proteins, the hyaladherins. *Current Opinion in Cell Biology*. **2**, 839-844, 1990.

Tsiganos, C.P., Hardingham, T.E. and Muir, H. Proteoglycans of cartilage: an assessment of their structure. *Biochimica et Biophysica Acta*. **229,** 529-534, 1971.

Turley, E.A. et.al. Hyaluronan and a cell-associated hyaluronan binding protein regulate the locomotion of ras-transformed cells. *The Journal of Cell Biology*. **112**(5), 1041-1047, 1991.

Turley, E.A., Bowman, P. and Kytryk, M.A. Effects of hyaluronate and hyaluronate binding proteins on cell motile and contact behavior. *J. Cell. Sci.* **78**, 133-145, 1985

Turley, E.A., Brassel, P. and Moore, D. A hyaluronan-binding protein shows a partial and temporally regulated codistributioni with actin on locomoting chick heart fibroblasts. *Experimental Cell Research.* **187**, 243-249, 1990.

Turner, M.R., Clough, G. and Michel, C.C. The effects of cationized ferritin and native ferritin upon the filtration coefficient of single frog capillaries. Evidence that proteins in the endothelial cell coat influence permeability. *Microvascular research.* **25**, 205-222, 1983.

Underhill, C.B. and Zhang, L. Analysis of hyaluronan using biotinylated hyaluronan binding proteins. *Methods in Molecular Biology.* **137,** 441-447.

Underhill, C.B., Thurn, A.L. and Lacy, B.E. Characterization and identification of the hyaluronate binding site from membranes of SV-3T3 cells. *The Journal of Biological Chemistry.* **260**(13), 8128-8133, 1985.

van den Berg, B.M. et.al. The endothelial glycocalyx protects against myocardial edema. *Circulation Research*. **92**, 592-594,2003.

van Haaren, P.M.A. et. al. Charge modification of the endothelial surface layer modulates the permeability barrier of isolated rat mesenteric small arteries. *Am. J. Physiol. Heart Circ.Physiol.* **289,** H2503-H2507, 2005.

vanTeeffelen, Jurgen W.G.F. et.al. Hyaluronidase treatment of coronary glycocalyx increases reactive hyperemia but not adenosine hyperemia in dog hearts. *Am J Physiol Heart Circ Physiol.* **289**, H2508-H2513, 2005.

Yanaki, T. and Yamaguchi, T. Temporary network formation of hyaluronate under a physiological condition. 1. Molecular-weight dependence. *Biopolymers.* **30**, 415-425, 1990,

Yang, B., Yang, B.L. and Goetinck, P.F. Biotinylated hyaluronic acid as a probe for identifying hyaluronic acid-binding proteins. *Analytical Biochemistry*. **228**, 299-306, 1995.

Zhu, W. et al. Determination of kinetic changes of aggrecan-hyaluronan interactions in solution from its rheological properties. *J. Biomechanics.* **27**(5), 571-579, 199.